

AD-A246 556



NAVAL POSTGRADUATE SCHOOL

Monterey, California



THESIS

Computation Of Acoustic
Normal Modes In The Ocean
Using Asymptotic Expansion Methods

by

Fernando M. M. Pimentel

September, 1991

Thesis Advisor:

Ching-Sang Chiu

Approved for public release; distribution is unlimited

92-04980



02 2 25 211

Unclassified

security classification of this page

REPORT DOCUMENTATION PAGE

1a Report Security Classification Unclassified			1b Restrictive Markings		
2a Security Classification Authority			3 Distribution Availability of Report		
2b Declassification Downgrading Schedule			Approved for public release; distribution is unlimited.		
4 Performing Organization Report Number(s)			5 Monitoring Organization Report Number(s)		
6a Name of Performing Organization Naval Postgraduate School		6b Office Symbol (if applicable) 35	7a Name of Monitoring Organization Naval Postgraduate School		
6c Address (city, state, and ZIP code) Monterey, CA 93943-5000			7b Address (city, state, and ZIP code) Monterey, CA 93943-5000		
8a Name of Funding Sponsoring Organization		8b Office Symbol (if applicable)	9 Procurement Instrument Identification Number		
8c Address (city, state, and ZIP code)			10 Source of Funding Numbers		
			Program Element No	Project No	Task No
			Work Unit Accession No		
11 Title (include security classification) COMPUTATION OF ACOUSTIC NORMAL MODES IN THE OCEAN USING ASYMPTOTIC EXPANSION METHODS					
12 Personal Author(s) Fernando M. M. Pimentel					
13a Type of Report Master's Thesis		13b Time Covered From To		14 Date of Report (year, month, day) September 1991	
				15 Page Count 77	
16 Supplementary Notation The views expressed in this thesis are those of the author and do not reflect the official policy or position of the Department of Defense or the U.S. Government.					
17 Cosati Codes			18 Subject Terms (continue on reverse if necessary and identify by block number)		
Field	Group	Subgroup	Acoustic normal modes by asymptotic expansion		
19 Abstract (continue on reverse if necessary and identify by block number)					
<p>In this thesis, the use of the Wentzel-Kramers-Brillouin (WKB) Theory to obtain the solution to the Helmholtz Equation governing the acoustic normal modes is examined. Specifically, uniformly valid WKB solutions for four classes of acoustic normal modes in the ocean are derived and the accuracy of the WKB approximation is tested against some exact solutions. It is found that this inherently high frequency technique has an appreciable accuracy even at a frequency of 1 Hz. A product of this thesis is a computer program that solves for the WKB modes for an arbitrary sound speed profile.</p>					
20 Distribution Availability of Abstract			21 Abstract Security Classification		
<input checked="" type="checkbox"/> unclassified unlimited <input type="checkbox"/> same as report <input type="checkbox"/> DTIC users			Unclassified		
22a Name of Responsible Individual Ching-Sang Chiu			22b Telephone (include Area code) (408) 646-3239		22c Office Symbol OC Ci

DD FORM 1473,84 MAR

83 APR edition may be used until exhausted
All other editions are obsolete

security classification of this page

Unclassified

Approved for public release; distribution is unlimited.

Computation Of Acoustic Normal Modes In The Ocean
Using Asymptotic Expansion Methods

by

Fernando M. M. Pimentel
Lieutenant, Portuguese Navy

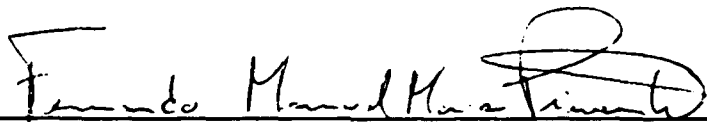
Submitted in partial fulfillment of the
requirements for the degree of

MASTER OF SCIENCE IN PHYSICAL OCEANOGRAPHY

from the

NAVAL POSTGRADUATE SCHOOL
September 1991

Author:

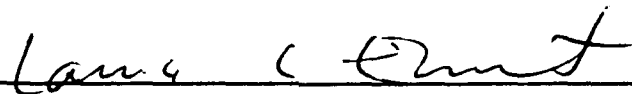


Fernando M. M. Pimentel

Approved by:



Ching-Sang Chiu, Thesis Advisor



Laura L. Ehret, Second Reader



Curtis A. Collins, Chairman,
Department of Oceanography

ABSTRACT

In this thesis, the use of the Wentzel-Kramers-Brillouin (WKB) Theory to obtain the solution to the Helmholtz Equation governing the acoustic normal modes is examined. Specifically, uniformly valid WKB solutions for four classes of acoustic normal modes in the ocean are derived and the accuracy of the WKB approximation is tested against some exact solutions. It is found that this inherently high frequency technique has an appreciable accuracy even at a frequency of 1 Hz. A product of this thesis is a computer program that solves for the WKB modes for an arbitrary sound speed profile.

Accession For	
NTIS GRA&I	<input checked="checked" type="checkbox"/>
DTIC TAB	<input type="checkbox"/>
Unannounced	<input type="checkbox"/>
Justification	
By	
Distribution/	
Availability Codes	
Dist	Avail and/or Special
A-1	

THESIS DISCLAIMER

The reader is cautioned that computer programs developed in this research may not have been exercised for all cases of interest. While every effort has been made, within the time available, to ensure that the programs are free of computational and logic errors, they cannot be considered validated. Any application of these programs without additional verification is at the risk of the user.

TABLE OF CONTENTS

I. INTRODUCTION	1
A. BACKGROUND	1
B. THE NORMAL MODE APPROACH	1
C. THESIS OBJECTIVES AND OUTLINE	2
II. WKB NORMAL MODES	4
A. FIRST ORDER WKB APPROXIMATION	4
1. The Mathematical Problem	4
2. Physical Approach	5
3. Basic Formulae	7
4. Comments	10
B. DETERMINATION OF WKB MODE PARAMETERS	10
1. General WKB Formulae	11
a. Class I: Pressure Release - Turning Point	11
b. Class II: Turning Point - Rigid Bottom	13
c. Class III: Turning Point - Turning Point	15
d. Class IV: Pressure Release - Rigid Bottom	18
2. Formulae Associated With Near-Boundary Turning Points	19
a. Class I	19
b. Class II	20
c. Class III	21
3. Criterion For Formulae Selection	21
4. Normalization	22
5. Parameter Storage	22
a. Classes I And II	22
b. Class III	22
c. Class IV	23
III. ACCURACY TEST	24
A. EXACT ANALYTICAL SOLUTIONS	24
1. Positive Exponential Profile	24

2. Negative Exponential Profile	26
3. Hyperbolic Profile	26
B. ANALYTICAL EVALUATION OF WKB PHASE INTEGRALS AND DERIVATIVES	28
1. Positive Exponential Profile	28
2. Negative Exponential Profile	30
3. Hyperbolic Profile	32
C. COMPARISON OF RESULTS	35
1. Horizontal Wavenumber Error Analysis	35
2. Errors In The Interference Distances	38
3. General Numerical Method	39
IV. CONCLUSIONS AND RECOMMENDATIONS	42
APPENDIX A. FIRST ORDER WKB THEORY	44
APPENDIX B. GENERAL BOUNDARY CONDITIONS	48
A. GENERAL FORMULA	48
B. TRAPPED MODES IN THE WATER COLUMN	50
1. Class I	50
2. Class II	51
3. Class III	52
4. Class IV	52
APPENDIX C. FORTRAN PROGRAM WKBGEN	54
A. PROGRAM DESCRIPTION	54
B. PROGRAM LISTING	54
REFERENCES	68
BIBLIOGRAPHY	69
INITIAL DISTRIBUTION LIST	70

I. INTRODUCTION

A. BACKGROUND

To model sound propagation in the ocean we can use several theories, namely Ray Theory, Parabolic Equation Approximation and Normal Modes. The Ray Theory solution is an asymptotic geometric-optics solution, obtainable using simple ray tracing techniques. It provides a simple physical description on how sound is transmitted underwater. However, it neglects sound diffraction and thus needs corrections near caustics and turning points. Such corrections can be very complicated mathematically. The Parabolic Equation method is less physical but is a full-wave solution. An asset of Parabolic Equation is its capability to handle variable bottom bathymetry well. Its limitation is that it does not accurately model sound energy propagating in steep angles. Normal Mode Theory gives a physical full-wave solution to the wave equation. It has some computational difficulties in handling range varying sound speed fields.

A computational difficulty associated with normal mode models applied to a range-dependent ocean is that the normal modes associated with a great number of profiles must be computed and the results stored. Large storage and processing time are required if straight-forward numerical methods such as finite differences are used to compute the normal modes (Chiu and Ehret, 1990). The use of finite differences methods requires the discretized mode functions and their eigenvalues at a great number of points to be stored. Moreover, at high frequencies these methods require the computation of eigenvectors and eigenvalues of large matrices, which can result in significant increases of processing time and numerical noise in the solution. In this thesis we examine an asymptotic expansion method that has the potential to overcome this difficulty. The method is called Wentzel-Kramers-Brillouin (WKB) theory.

B. THE NORMAL MODE APPROACH

The wave equation governing the sound pressure p in the ocean is

$$\frac{\partial^2 p}{\partial t^2} = c^2 \nabla^2 p$$

where $c = c(z; r, \theta)$ is the sound speed and z is the vertical coordinate, r the range and θ the azimuthal angle. In the three-dimensional coupled mode model of Chiu and Ehret

(1990), the pressure is expressed as a linear combination of the local normal modes Z_n such that

$$p(r, \theta, z) = \sum_{n=1}^{\infty} Z_n(z; r, \theta) P_n(r, \theta) T(t) .$$

For a harmonic frequency time dependence

$$T(t) = e^{i\omega t}$$

where ω is the acoustic angular frequency, the local modes at each horizontal location (r, θ) are required to satisfy

$$\frac{\partial^2 Z_n}{\partial z^2} + \left[\left(\frac{\omega}{c} \right)^2 - \kappa_n^2 \right] Z_n = 0$$

and the appropriate boundary conditions. This equation is usually known as the Helmholtz Equation. The constant κ_n is the horizontal component of the wavenumber vector whose magnitude is given by

$$\kappa = \frac{\omega}{c} .$$

In general, there are many possible values of κ_n (eigenvalues) satisfying the Helmholtz Equation. For each κ_n there is an associated mode Z_n (eigenfunction). In a range-dependent sound speed field this eigenvalue-eigenfunction problem must be solved at a great number of horizontal grid points.

C. THESIS OBJECTIVES AND OUTLINE

The main objective of this thesis is to examine the use of the WKB theory to solve the Helmholtz Equation governing the acoustic normal modes. This includes:

1. the development of the various WKB formulae for the four classes of normal modes which can exist in single duct/channel environments,
2. the parameterization of each class of normal modes using a minimum number of parameters,
3. the quantification of errors in the WKB solution through comparisons to three exact solutions.

A product coming out of this thesis is a computer program solving for the mode parameters for an arbitrary sound speed profile. The incorporation of this code in the

three-dimensional coupled mode model of Chiu and Ehret (1990) is expected to result in significant savings of processing time and computer storage.

In Chapter II, the WKB formulae are developed. The four types of normal modes are discussed. In Chapter III, the normal modes and their eigenvalues for three abstract sound speed profiles are solved exactly. The WKB results are then compared to the exact solutions for an error analysis. Conclusions are given in Chapter IV.

II. WKB NORMAL MODES

A. FIRST ORDER WKB APPROXIMATION

1. The Mathematical Problem

The WKB approximation to the solution of a differential equation is an asymptotic expansion method applicable to a large range of equations. It is named after Wentzel, Kramers and Brillouin who used it separately but at about the same time in 1926. However the principle of this technique was developed by Liouville and Green in 1837. It was also used by Rayleigh (1912), Gans (1915) and Jeffreys (1924), among others. The WKB method is also known as the Liouville-Green or WKBJ approximation (the letter J is used to honour Jeffreys' contribution).

To compute the acoustic normal modes the equation to be solved is the Helmholtz Equation

$$\frac{d^2 Z_n}{dz^2} + \kappa_{zn}^2 Z_n = 0 \quad (1)$$

where

$$\kappa_{zn}^2 = \frac{\omega^2}{c^2} - \kappa_n^2$$

is the vertical wavenumber, Z_n is the n^{th} normal mode, z is the vertical coordinate, ω the acoustic angular frequency, $c = c(z)$ the sound speed and κ_n the horizontal wavenumber. With a pressure release surface and a rigid bottom the appropriate boundary conditions are

$$Z_n = 0 \text{ at the surface} \quad (2)$$

$$\frac{dZ_n}{dz} = 0 \text{ at the bottom} \quad (3)$$

Normal modes subjected to general boundary conditions are discussed in Appendix B. Note that, in (1) through (3), we have suppressed the dependence in range which has no effect on the local modes. Equation (1), together with (2) and (3), is a Sturm-Liouville

problem where the Z_n 's are the eigenfunctions and the κ_n 's are the eigenvalues. The eigenfunctions can be normalized using a normalization constant C_n such that

$$\bar{Z}_n = C_n Z_n \quad (4)$$

where

$$\int \bar{Z}_n \bar{Z}_m dz = \delta_{nm} \quad (5)$$

Note that the integration is over the entire depth in (5), δ_{nm} is the Kronecker Delta, and Z_n and Z_m are orthogonal for $n \neq m$.

There are several ways to obtain the first order WKB solution. A physical approach is to consider the transmission of plane waves through a layered medium. The WKB solution is obtained as we let the the layer thickness approach zero. This physical approach will be discussed next.

2. Physical Approach

In each isospeed layer the solution to the Helmholtz Equation is given by

$$Z_n^j \propto e^{\pm i \kappa_{zn}^j z}$$

where κ_{zn}^j is the vertical wavenumber in the j^{th} layer. The transmission coefficient from layer j to layer $j+1$ is given by (Kinsler et al., 1982)

$$T_{jj+1} = 2 \frac{\kappa_{zn}^j}{\kappa_{zn}^j + \kappa_{zn}^{j+1}}$$

or

$$T_{jj+1} = \frac{1}{1 + \frac{1}{2} \frac{\Delta \kappa_{zn}^j}{\kappa_{zn}^j}}$$

where $\Delta \kappa_{zn}^j = \kappa_{zn}^{j+1} - \kappa_{zn}^j$. With $\frac{\Delta \kappa_{zn}^j}{\kappa_{zn}^j} \ll 1$ we get

$$T_{jj+1} = e^{-\frac{1}{2} \frac{\Delta \kappa_{zn}^j}{\kappa_{zn}^j}} \quad .$$

By letting $|Z_n| = 1$ we have

$$Z_n^j = \left(\prod_{m=1}^{j-1} T_{m, m+1} \right) e^{\pm i \sum_{m=1}^j \kappa_{zn}^m \Delta z_m} = e^{-\frac{1}{2} \sum_{m=1}^{j-1} \frac{\Delta \kappa_{zn}^m}{\kappa_{zn}^m}} e^{\pm i \sum_{m=1}^j \kappa_{zn}^m \Delta z_m}$$

where Z_n^j is the value at the interface of the j^{th} layer and the $(j+1)^{\text{th}}$ layer and Δz_m is the thickness of the m^{th} layer. Taking the thickness of the layers to zero we have

$$Z_n(z) = e^{-\frac{1}{2} \int_{z_c}^{z_n} \frac{d\kappa_{zn}}{\kappa_{zn}}} e^{\pm i \int_{z_1}^z \kappa_{zn} dz},$$

or

$$Z_n(z) = \frac{\sqrt{\kappa_c}}{\sqrt{\kappa_{zn}}} e^{\pm i \phi}$$

where κ_c is the vertical wavenumber at $z = z_1$ and

$$\phi = \int_{z_1}^z |\kappa_{zn}| dz.$$

The vertical wavenumber κ_{zn} generally can take on real or imaginary values. If κ_{zn} is real, i.e., $\kappa_{zn}^2 > 0$, the solution is

$$Z_n(z) = \frac{a' e^{i\phi} + b' e^{-i\phi}}{\sqrt{\kappa_{zn}}}$$

or

$$Z_n(z) = \frac{a \cos \phi + b \sin \phi}{\sqrt{\kappa_{zn}}} \quad (6)$$

where a' and b' or a and b are constants to be determined by normalization and the boundary conditions. On the other hand if κ_{zn} is purely imaginary, i.e., $\kappa_{zn}^2 < 0$, we have

$$Z_n(z) = \frac{a e^{\phi} + b e^{-\phi}}{\sqrt{|\kappa_{zn}|}} \quad (7)$$

These last two formulae are precisely the WKB solution to the Helmholtz Equation in regions not close to a point where $\kappa_{zn} = 0$ (i.e., a turning point).

3. Basic Formulae

By substituting the WKB solutions (6) or (7) in the Helmholtz Equation, one can easily show that they are exact solutions if

$$r(z) = \frac{3}{4} \frac{1}{\kappa_{zn}^4} \left(\frac{d\kappa_{zn}}{dz} \right)^2 - \frac{1}{2} \frac{1}{\kappa_{zn}^3} \frac{d^2\kappa_{zn}}{dz^2} = 0 .$$

Therefore, if $|r(z)| \ll 1$ the WKB solutions (6) and (7) are good approximations to the exact solution for $\kappa_{zn}^2 > 0$ and $\kappa_{zn}^2 < 0$, respectively. In Appendix A a more detailed and mathematical derivation of the WKB solution and its validity is presented. Let us call these solutions the first order WKB approximation. But (6) and (7) are not valid when $\kappa_{zn}^2 = 0$ (i. e., at a turning point) or even in a region where $\kappa_{zn}^2 \sim 0$. We need a solution valid at and near the turning point (i.e., in the critical region) to make the liaison between the oscillatory region ($\kappa_{zn}^2 \gg 0$) and the exponential region ($\kappa_{zn}^2 \ll 0$).

Let us suppose that there is a turning point at $z=0$ and $\kappa_{zn}^2 > 0$ for $z > 0$ and $\kappa_{zn}^2 < 0$ for $z < 0$. Consistent with a first order approximation, let us assume that near the turning point $\kappa_{zn}^2 = \gamma z$ where

$$\gamma = \left(\frac{d\kappa_{zn}^2}{dz} \right)_{z=0} .$$

With a change of coordinate

$$\zeta = -\gamma^{1/3} z ,$$

the Helmholtz Equation becomes

$$\frac{d^2 Z_n}{d\zeta^2} - \zeta Z_n = 0$$

which is the Airy Equation with the general solution given by

$$Z_n(\zeta) = aAi(\zeta) + bBi(\zeta) .$$

The Airy Functions can be expressed as, with $\zeta \geq 0$,

$$Ai(-\zeta) = \frac{\sqrt{\zeta}}{3} \left[J_{-1/3} \left(\frac{2}{3} \zeta^{3/2} \right) + J_{1/3} \left(\frac{2}{3} \zeta^{3/2} \right) \right]$$

$$Bi(-\zeta) = \sqrt{\frac{\zeta}{3}} \left[J_{-1/3} \left(\frac{2}{3} \zeta^{3/2} \right) - J_{1/3} \left(\frac{2}{3} \zeta^{3/2} \right) \right]$$

$$Ai(\zeta) = \frac{\sqrt{\zeta}}{3} \left[I_{-1/3} \left(\frac{2}{3} \zeta^{3/2} \right) - I_{1/3} \left(\frac{2}{3} \zeta^{3/2} \right) \right]$$

$$Bi(\zeta) = \sqrt{\frac{\zeta}{3}} \left[I_{-1/3} \left(\frac{2}{3} \zeta^{3/2} \right) + I_{1/3} \left(\frac{2}{3} \zeta^{3/2} \right) \right]$$

where J 's are Bessel Functions and I 's are Modified Bessel Functions.

Now we have a complete set of first order approximate solutions covering the entire range of κ_{zn}^2 . Summarizing, we have:

(a) in the oscillatory region ($\kappa_{zn}^2 \gg 0$)

$$Z_n(z) = \frac{a_1 \sin \phi + b_1 \cos \phi}{\sqrt{\kappa_{zn}}} , \quad (8)$$

(b) in the critical region ($\kappa_{zn}^2 \sim 0$)

$$\kappa_{zn}^2 = \gamma z$$

$$\zeta = -\gamma^{1/3} z$$

$$Z_n(z) = a_2 Ai(\zeta) + b_2 Bi(\zeta) , \quad (9)$$

(c) in the exponential region ($\kappa_{zn}^2 \ll 0$)

$$Z_n(z) = \frac{a_3 e^{-\phi} + b_3 e^{\phi}}{\sqrt{|\kappa_{zn}|}} . \quad (10)$$

To assure continuity in $Z_n(z)$ at the boundaries between regions, we must relate the constants a , and b , carefully. An asymptotic expansion of the critical region solution for large positive values of κ_{zn}^2 (or $-\zeta > 1$) must match the solution in the oscillatory region and for large negative values of κ_{zn}^2 (or $\zeta > 1$) must match the solution in the exponential region. The connection formulae between the three regions are given by

$$\frac{1}{\sqrt{|\kappa_{zn}|}} \frac{e^{-\phi}}{2} \leftarrow \sigma Ai(\zeta) \rightarrow \frac{1}{\sqrt{\kappa_{zn}}} \sin(\phi + \frac{\pi}{4})$$

$$\frac{1}{\sqrt{|\kappa_{zn}|}} e^{\phi} \leftarrow \sigma Bi(\zeta) \rightarrow \frac{1}{\sqrt{\kappa_{zn}}} \cos(\phi + \frac{\pi}{4})$$

where the left sides match the Airy Functions for $\kappa_{zn}^2 \ll 0$ and the right sides match for $\kappa_{zn}^2 \gg 0$ (Bender and Orszag, 1978) with

$$\sigma = \sqrt{\pi} \gamma^{-1/6} .$$

Therefore, (8), (9) and (10) can be recast respectively as

(a) oscillatory region solution

$$Z_n(z) = \frac{a \sin(\phi + \frac{\pi}{4}) + b \cos(\phi + \frac{\pi}{4})}{\sqrt{\kappa_{zn}}} , \quad (11.a)$$

(b) critical region solution

$$Z_n(z) = a\sigma Ai(\zeta) + b\sigma Bi(\zeta) , \quad (11.b)$$

(c) exponential region solution

$$Z_n(z) = \frac{(a/2)e^{-\phi} + be^{\phi}}{\sqrt{|\kappa_{zn}|}} . \quad (11.c)$$

The constants κ_n , a and b are determined by normalization and the boundary conditions. The equations for the eigenvalues κ_n , i.e., the characteristic equations, involve the solution in the oscillatory region (11.a), as will be discussed later.

Equations (11.a,b,c) are not easy to use in the computation of normal mode shapes. Where does one stop with one formula and start with another? This problem is avoided if, after the determination of the eigenvalue κ_n and the constants a and b , the computation of the normal mode is done using the Langer Formula (Nayfeh, 1973; Bender and Orszag, 1978)

$$Z_n(z) = 2\sqrt{\pi} \left(\frac{2}{3} |\phi| \right)^{1/6} \frac{1}{\sqrt{|\kappa_{zn}|}} \left\{ a Ai \left[s \left(\frac{3}{2} \phi \right)^{2/3} \right] + b Bi \left[s \left(\frac{3}{2} \phi \right)^{2/3} \right] \right\} \quad (12)$$

with

$$\phi = \int_0^z |\kappa_{zn}| dz$$

and

$$s = -z/|z| \quad .$$

This formula has the advantage of giving a single and continuous solution for the entire range of κ_{zn}^2 . Bender and Orszag (1978) have shown that for $\kappa_{zn}^2 \sim 0$ and $\kappa_{zn}^2 = \gamma z$ the formula gives exactly (11.b), for $\kappa_{zn}^2 \gg 0$ it asymptotically approaches (11.a) and for $\kappa_{zn}^2 \ll 0$ it approaches (11.c).

In retrospect, in order to obtain the first order WKB solution, an algorithm must include the following steps:

(a) application of a boundary condition to (11.a,b,c) to get the relationship between the constants a and b ;

(b) application of the other boundary condition to (11.a) to get the characteristic equation;

(c) with (12) compute $Z_n(z)$;

(d) with (4) and (5) normalize $Z_n(z)$.

4. Comments

The WKB solution is a high frequency approximation. This means that it gets better as the frequency gets higher. It must be noted that, although Normal Modes are a full-wave exact solution to the wave equation, the WKB modes are approximate solutions and their accuracy is frequency dependent.

B. DETERMINATION OF WKB MODE PARAMETERS

Now that we have a uniformly-valid first order solution to the Helmholtz Equation, we are ready to apply the boundary conditions to get expressions for the κ_n 's and the constants a and b (or their equivalents). There are four classes of normal modes to consider. Each class has different mathematical expressions for the mode parameters (a , b , or their equivalents, and κ_n). Therefore, for an arbitrary sound speed profile the first procedure for normal mode calculation is to determine which class each mode falls into and then go through the steps described at the end of the previous section.

1. General WKB Formulae

We start by deriving the more general formulae which are applicable to modes that do not have turning points in close vicinity of the boundaries.

a. Class I: Pressure Release - Turning Point

First let us consider a mode whose oscillatory region is bounded by a turning point at the depth $z = \hat{z}$ and the surface ($z = 0$). With the bottom at $z = H$, the boundary conditions are

$$Z_n(0) = 0 \quad (13)$$

$$\frac{dZ_n}{dz}(H) = 0 \quad (14)$$

We will call this class of modes as PR-TP (Pressure Release - Turning Point).

In the exponential region ($\hat{z} \ll z \leq H$), the WKB solution can be recast as

$$Z_n \propto \frac{\cosh(\phi - \phi_b)}{\sqrt{|\kappa_{zn}|}} \quad (15)$$

with

$$\phi = \int_{\hat{z}}^z |\kappa_{zn}| dz.$$

In order to satisfy the boundary condition (14), ϕ_b must be given by

$$\phi_b = \int_{\hat{z}}^H |\kappa_{zn}| dz - \tanh^{-1} \left(\frac{1}{2|\kappa_{zn}|^2} \frac{d|\kappa_{zn}|}{dz} \right)_{z=H}.$$

We need to connect (15) to the solutions in the critical and oscillatory regions next. After application of the connection formulae, the results in the three regions are:

(a) exponential region

$$Z_n = \frac{1}{\sqrt{|\kappa_{zn}|}} \cosh(\phi - \phi_b), \quad (16.a)$$

(b) critical region

$$\kappa_{zn}^2 = \gamma(\hat{z} - z)$$

$$\zeta = -\gamma^{1/3}(\hat{z} - z)$$

$$Z_n = e^{\phi_b} \sigma Ai(\zeta) + \frac{e^{-\phi_b}}{2} \sigma Bi(\zeta) , \quad (16.b)$$

(c) oscillatory region

$$Z_n = \frac{e^{\phi_b}}{\sqrt{\kappa_{zn}}} \sin\left(\phi + \frac{\pi}{4}\right) + \frac{e^{-\phi_b}}{2\sqrt{\kappa_{zn}}} \cos\left(\phi + \frac{\pi}{4}\right) \quad (16.c)$$

with

$$\phi = \int_z^{\hat{z}} |\kappa_{zn}| dz$$

in this region. The corresponding Langer Formula that asymptotically matches (16.a,b,c) is

$$Z_n = 2\sqrt{\pi} \left(\frac{2}{3} |\phi|\right)^{1/6} \frac{1}{\sqrt{|\kappa_{zn}|}} \left\{ e^{\phi_b} Ai\left[s\left(\frac{3}{2}\phi\right)^{2/3}\right] + \frac{e^{-\phi_b}}{2} Bi\left[s\left(\frac{3}{2}\phi\right)^{2/3}\right] \right\} \quad (17)$$

with

$$s = \frac{z - \hat{z}}{|z - \hat{z}|}$$

and

$$\phi = \int_{\hat{z}}^z |\kappa_{zn}| dz.$$

As the oscillatory region solution must satisfy the surface boundary condition, we have

$$\frac{e^{-\phi_b}}{2\sqrt{\kappa_{zn}}} \cos\left(\int_0^{\hat{z}} \kappa_{zn} dz + \frac{\pi}{4}\right) + \frac{e^{\phi_b}}{\sqrt{\kappa_{zn}}} \sin\left(\int_0^{\hat{z}} \kappa_{zn} dz + \frac{\pi}{4}\right) = 0 , \quad (18)$$

or

$$\int_0^{\hat{z}} \kappa_{zn} dz = \left(n - \frac{1}{4}\right) \pi - \tan^{-1} \left(\frac{e^{-\phi_b}}{2e^{\phi_b}} \right) .$$

This is the characteristic equation for PR - TP normal modes. The solutions to the characteristic equation give the eigenvalues κ_n 's.

b. Class II: Turning Point - Rigid Bottom

The next class of normal modes to be considered has the oscillatory region between a turning point and the bottom. It will be called TP-RB (Turning Point - Rigid Bottom). For this class, let us express the solution in the exponential region, $0 \leq z \ll \hat{z}$, as

$$Z_n \propto \frac{1}{\sqrt{|\kappa_{zn}|}} \sinh(\phi - \phi_s)$$

with

$$\phi = \int_z^{\hat{z}} |\kappa_{zn}| dz$$

and

$$\phi_s = \int_0^{\hat{z}} |\kappa_{zn}| dz.$$

Using the connection formulae, we get for the three regions:

(a) Exponential Region

$$Z_n = - \frac{1}{\sqrt{|\kappa_{zn}|}} \sinh(\phi - \phi_s)$$

(b) Critical Region

$$\kappa_{zn}^2 = \gamma(z - \hat{z})$$

$$\zeta = -\gamma^{1/3}(z - \hat{z})$$

$$Z_n = e^{\phi_r} \sigma Ai(\zeta) - \frac{e^{-\phi_r}}{2} \sigma Bi(\zeta)$$

(c) Oscillatory Region

$$Z_n = \frac{e^{\phi_s}}{\sqrt{\kappa_{zn}}} \sin\left(\phi + \frac{\pi}{4}\right) - \frac{e^{-\phi_s}}{2\sqrt{\kappa_{zn}}} \cos\left(\phi + \frac{\pi}{4}\right) \quad (19)$$

with

$$\phi = \int_{\hat{z}}^z |\kappa_{zn}| dz$$

in this region ($\hat{z} \ll z \leq H$). The appropriate Langer Formula for this class is

$$Z_n = 2\sqrt{\pi} \left(\frac{2}{3} |\phi|\right)^{1/6} \frac{1}{\sqrt{|\kappa_{zn}|}} \left\{ e^{\phi_s} Ai \left[s \left(\frac{3}{2} \phi \right)^{2/3} \right] - \frac{e^{-\phi_s}}{2} Bi \left[s \left(\frac{3}{2} \phi \right)^{2/3} \right] \right\} \quad (20)$$

where

$$s = - \frac{z - \hat{z}}{|z - \hat{z}|}$$

and

$$\phi = \int_{\hat{z}}^z |\kappa_{zn}| dz.$$

Equation (19) must satisfy the bottom boundary condition (14), therefore, we have

$$\sin \left[\int_{\hat{z}}^H \kappa_{zn} dz + \frac{\pi}{4} + \tan^{-1} \left(\frac{e^{\phi_s} + \frac{D}{2} e^{-\phi_s}}{\frac{e^{-\phi_s}}{2} - D e^{\phi_s}} \right) \right] = 0 \quad (21)$$

where

$$D = \left(\frac{1}{2\kappa_{zn}^2} \frac{d\kappa_{zn}}{dz} \right)_{z=H} \quad (22)$$

It follows from (21) that the characteristic equation for TP - RB is

$$\int_{\hat{z}}^H \kappa_{zn} dz = \left(n - \frac{1}{4}\right) \pi - \tan^{-1} \left(\frac{e^{\phi_s} + \frac{D}{2} e^{-\phi_s}}{\frac{e^{-\phi_s}}{2} - D e^{\phi_s}} \right)$$

for $D < 0$, and

$$\int_{\hat{z}}^H \kappa_{zn} dz = \left(n - \frac{5}{4}\right) \pi - \tan^{-1} \left(\frac{e^{\phi_s} + \frac{D}{2} e^{-\phi_s}}{\frac{e^{-\phi_s}}{2} - D e^{\phi_s}} \right)$$

for $D > 0$.

c. Class III: Turning Point - Turning Point

The third class of modes has the oscillatory region between two turning points, at $z = \hat{z}_1$ and $z = \hat{z}_2$ with $\hat{z}_1 < \hat{z}_2$. They will be referred as TP-TP (Turning Point - Turning Point).

Let us express the solution in the exponential region near the surface, $0 \leq z \ll \hat{z}_1$, as

$$Z_n = - \frac{c_1}{\sqrt{|\kappa_{zn}|}} \sinh(\phi_1^- - \phi_s)$$

where

$$\phi_1^- = \int_{\hat{z}}^{\hat{z}_1} |\kappa_{zn}| dz$$

and

$$\phi_s = \int_0^{\hat{z}_1} |\kappa_{zn}| dz,$$

and the solution in the exponential region near the bottom, $\hat{z}_2 \ll z \leq H$, as

$$Z_n = \frac{c_2}{\sqrt{|\kappa_{zn}|}} \cosh(\phi_2^+ - \phi_b)$$

with

$$\phi_2^+ = \int_{\hat{z}_2}^z |\kappa_{zn}| dz$$

and

$$\phi_b = \int_{\hat{z}_2}^H |\kappa_{zn}| dz - \tanh^{-1} \left(\frac{1}{2|\kappa_{zn}|^2} \frac{d|\kappa_{zn}|}{dz} \right)_{z=H}.$$

In addition, let us express the solution in the critical region centered at $z = \hat{z}_1$ as

$$Z_n = c_1 e^{\phi_1 \sigma_1} Ai(\zeta_1) - \frac{c_1}{2} e^{-\phi_1 \sigma_1} Bi(\zeta_1) \quad (23)$$

with

$$\kappa_{zn}^2 = \gamma_1 (z - \hat{z}_1),$$

$$\sigma_1 = \sqrt{\pi} \gamma_1^{-1/6}$$

and

$$\zeta_1 = -\gamma_1^{1/3} (z - \hat{z}_1),$$

and in the other critical region, centered at $z = \hat{z}_2$, as

$$Z_n = c_2 e^{\phi_b \sigma_2} Ai(\zeta_2) + \frac{c_2}{2} e^{-\phi_b \sigma_2} Bi(\zeta_2) \quad (24)$$

with

$$\kappa_{zn}^2 = \gamma_2 (\hat{z}_2 - z),$$

$$\sigma_2 = \sqrt{\pi} \gamma_2^{-1/6}$$

and

$$\zeta_2 = -\gamma_2^{1/3} (\hat{z}_2 - z).$$

By letting

$$c_1 = \frac{1}{\sqrt{e^{2\phi_1} + \frac{e^{-2\phi_1}}{4}}}$$

and connecting (23) to the solution in the oscillatory region $\hat{z}_1 \ll z \ll \hat{z}_2$, we get

$$Z_n = \frac{1}{\sqrt{\kappa_{zn}}} \sin\left(\phi_1^+ + \frac{\pi}{4} - \alpha_1\right) \quad (25)$$

where

$$\phi_1^+ = \int_{\hat{z}_1}^z |\kappa_{zn}| dz$$

and

$$\alpha_1 = \tan^{-1}\left(\frac{e^{-\phi_1}}{2e^{\phi_1}}\right).$$

Note that, in obtaining (25), the trigonometric identity

$$a \cos \theta + b \sin \theta = \sqrt{a^2 + b^2} \sin\left(\theta + \tan^{-1} \frac{a}{b}\right) \quad (26)$$

has been used. In the same way, by letting

$$c_2 = \frac{1}{\sqrt{e^{2\phi_2} + \frac{e^{-2\phi_2}}{4}}}$$

and connecting (24) to the oscillatory region solution we get

$$Z_n = \frac{1}{\sqrt{\kappa_{zn}}} \sin\left(\phi_2^- + \frac{\pi}{4} + \alpha_2\right) \quad (27)$$

where

$$\phi_2^- = \int_z^{\hat{z}_2} |\kappa_{zn}| dz$$

and

$$\alpha_2 = \tan^{-1} \left(\frac{e^{-\phi_b}}{2e^{\phi_b}} \right).$$

Realizing that the two solutions, (25) and (27), in the oscillatory region must be identical, we obtain

$$\sin \left(\phi_1^+ + \frac{\pi}{4} - \alpha_1 \right) = \sin \left(\phi_2^- + \frac{\pi}{4} + \alpha_2 \right) . \quad (28)$$

Using (28), the characteristic equation for this class of normal modes is obtained:

$$\int_{\hat{z}_1}^{\hat{z}_2} \kappa_{zn} dz = \left(n - \frac{1}{2} \right) \pi + \alpha_1 - \alpha_2 .$$

To compute the normal mode we can use (20) for $z \leq \hat{z}_1$ and (17) for $z \geq \hat{z}_2$.

d. Class IV: Pressure Release - Rigid Bottom

Finally, we must consider modes having no turning points. We call this class PR-RB (Pressure Release - Rigid Bottom). Here we express the solution, which is always oscillatory, as

$$Z_n \propto \frac{a}{\sqrt{\kappa_{zn}}} \sin \phi + \frac{b}{\sqrt{\kappa_{zn}}} \cos \phi \quad (29)$$

with

$$\phi = \int_0^z |\kappa_{zn}| dz .$$

Since the surface boundary condition must be satisfied, we must have $b = 0$, and hence

$$Z_n = \frac{1}{\sqrt{\kappa_{zn}}} \sin \phi . \quad (30)$$

On the other hand, (30) must satisfy the bottom boundary condition (14) and this leads to the characteristic equation for the PR - RB modes:

$$\int_0^H \kappa_{zn} dz = n\pi - \tan^{-1}\left(\frac{1}{D}\right)$$

for $D > 0$, and

$$\int_0^H \kappa_{zn} dz = n\pi + \tan^{-1}\left(\frac{1}{D}\right)$$

for $D < 0$, where D is given in (22).

2. Formulae Associated With Near-Boundary Turning Points

In our derivation of the formulae in the previous section, we have applied the boundary conditions to the oscillatory or exponential region solutions, assuming that the boundaries are nowhere close to any turning point. In the special case that a boundary lies inside a critical region, the respective boundary condition must be applied to the critical region solution instead. Different formulae associated with the first three classes of modes for this special case will be derived next.

a. Class I

PR - TP modes have lower turning points. Since the solution in the critical region must now satisfy the bottom boundary condition we obtain

$$Z_n = Bi'(\zeta_H)\sigma Ai(\zeta) - Ai'(\zeta_H)\sigma Bi(\zeta)$$

where

$$\zeta_H = \gamma^{1/3}(H - \hat{z})$$

and

$$\gamma = -\left(\frac{d\kappa_{zn}^2}{dz}\right)_{z=\hat{z}}$$

Ai' and Bi' are the derivatives of the Airy Functions with respect to ζ and are defined by (with $\zeta \geq 0$)

$$Ai'(-\zeta) = -\frac{1}{3}\zeta \left[J_{-2/3}\left(\frac{2}{3}\zeta^{3/2}\right) - J_{2/3}\left(\frac{2}{3}\zeta^{3/2}\right) \right]$$

$$Bi'(-\zeta) = \frac{1}{\sqrt{3}} \zeta \left[J_{-2/3} \left(\frac{2}{3} \zeta^{3/2} \right) + J_{2/3} \left(\frac{2}{3} \zeta^{3/2} \right) \right]$$

$$Ai'(\zeta) = -\frac{1}{3} \zeta \left[I_{-2/3} \left(\frac{2}{3} \zeta^{3/2} \right) - I_{2/3} \left(\frac{2}{3} \zeta^{3/2} \right) \right]$$

$$Bi'(\zeta) = \frac{1}{\sqrt{3}} \zeta \left[I_{-2/3} \left(\frac{2}{3} \zeta^{3/2} \right) + I_{2/3} \left(\frac{2}{3} \zeta^{3/2} \right) \right] .$$

Defining

$$A_1 = Bi'(\zeta_H)$$

and

$$B_1 = Ai'(\zeta_H)$$

and applying the connection formulae, the solution in the oscillatory region becomes

$$Z_n = \frac{A_1}{\sqrt{\kappa_{zn}}} \sin \left(\phi + \frac{\pi}{4} \right) - \frac{B_1}{\sqrt{\kappa_{zn}}} \cos \left(\phi + \frac{\pi}{4} \right) .$$

An application of the surface boundary condition gives the following characteristic equation:

$$\int_0^{\hat{z}} \kappa_{zn} dz = \left(n - \frac{1}{4} \right) \pi + \tan^{-1} \left(\frac{B_1}{A_1} \right) .$$

b. Class II

TP - RB modes have upper turning points. To satisfy the surface boundary condition, we require the solution in the critical region to vanish at the surface, i. e.,

$$Z_n = Bi(\zeta_S) \sigma Ai(\zeta) - Ai(\zeta_S) \sigma Bi(\zeta)$$

with

$$\zeta_S = \gamma^{1/3} \hat{z}$$

and

$$\gamma = \left(\frac{d\kappa_{zn}^2}{dz} \right)_{z=\hat{z}} .$$

Defining

$$A_2 = Bi(\zeta_S)$$

and

$$B_2 = Ai(\zeta_S)$$

and applying the connection formulae, the solution in the oscillatory region becomes

$$Z_n = \frac{A_2}{\sqrt{\kappa_{zn}}} \sin\left(\phi + \frac{\pi}{4}\right) - \frac{B_2}{\sqrt{\kappa_{zn}}} \cos\left(\phi + \frac{\pi}{4}\right) .$$

The subsequent application of the bottom boundary condition leads to the following characteristic equation :

$$\int_{\hat{z}}^H \kappa_{zn} dz = \left(n - \frac{1}{4}\right) \pi - \tan^{-1} \left(\frac{A_2 + DB_2}{B_2 - DA_2} \right)$$

for $D < 0$, and

$$\int_{\hat{z}}^H \kappa_{zn} dz = \left(n - \frac{5}{4}\right) \pi - \tan^{-1} \left(\frac{A_2 + DB_2}{B_2 - DA_2} \right)$$

for $D > 0$, where D is defined in (22).

c. Class III

With the above results, we can easily see that only two modifications in the general formulae for TP - TP modes are required. These include replacing e^{ϕ_s} by A_1 and $\frac{e^{-\phi_s}}{2}$ by B_1 , if the upper turning point is close to the surface, and e^{ϕ_b} by A_1 and $-\frac{e^{-\phi_b}}{2}$ by B_1 , if the lower turning point is near the bottom.

3. Criterion For Formulae Selection

We must define a criterion for switching from the general formulae to the formulae associated with near-boundary turning points. It was found by Bender and Orszag (1978) that the critical region extends on each side of the turning point until

$|\zeta| \sim 1$. In accordance, we will use the general formulae unless the distance between a turning point and a boundary corresponds to values of $|\zeta|$ smaller than 1.

4. Normalization

Once normal mode parameters are computed using the appropriate formulae including the characteristic equations, the normalization of the normal modes can be achieved by numerical integration over depth. The normalized modes (\bar{Z}_n 's) are related to the Z_n 's by

$$\bar{Z}_n = C_n Z_n$$

with

$$\frac{1}{C_n^2} = \int_0^H Z_n^2 dz .$$

5. Parameter Storage

We now define the necessary parameters required to completely characterize each mode. The first parameter is obviously the class number. By checking the formulae developed in the previous sections it is seen that all the constants (ϕ_s , ϕ_b , D , etc.) can be computed from the horizontal wavenumber, the depths of the turning points and the depth of the ocean. Therefore, the parameters required to parameterize each class of modes are:

a. Classes I And II

1. Class number
2. Horizontal wavenumber
3. Normalization constant
4. Depth of the turning point

b. Class III

1. Class number
2. Horizontal wavenumber
3. Normalization constant
4. Depth of the upper turning point
5. Depth of the lower turning point

c. Class IV

1. Class number
2. Horizontal wavenumber
3. Normalization constant

III. ACCURACY TEST

A. EXACT ANALYTICAL SOLUTIONS

To quantify the accuracy of the first order WKB approximation, we will compare the WKB solutions to exact analytical solutions to the Helmholtz Equation for three abstract sound speed profiles. The exact solutions are derived in this section. We use as boundary conditions pressure release surface and rigid bottom for all three cases.

1. Positive Exponential Profile

In this upward refractive profile, sound speed increases exponentially with the depth and is given by

$$c(z) = c_0 e^{\beta z}$$

where β is a constant. The surface is at $z = 0$ and the bottom at $z = H$. The Helmholtz Equation is

$$\frac{d^2 Z_n}{dz^2} + \left[\left(\frac{\omega}{c_0 e^{\beta z}} \right)^2 - \kappa_n^2 \right] Z_n = 0$$

or

$$\frac{d^2 Z_n}{dz^2} + (\kappa_0^2 e^{-2\beta z} - \kappa_n^2) Z_n = 0 \quad (31)$$

with $\kappa_0^2 = \frac{\omega^2}{c_0^2}$.

With a change of variable

$$\chi = e^{-\beta z} ,$$

(31) becomes

$$\beta^2 \chi \frac{d}{d\chi} \left(\chi \frac{dZ_n}{dz} \right) + (\kappa_0^2 \chi^2 - \kappa_n^2) Z_n = 0 .$$

After division by $\beta^2 \chi^2$ and using

$$\alpha_0 = \frac{\kappa_0}{\beta} \quad (32)$$

and

$$\alpha_n = \frac{\kappa_n}{\beta} \quad , \quad (33)$$

we obtain

$$\frac{1}{\chi} \frac{d}{d\chi} \left(\chi \frac{dZ_n}{d\chi} \right) + \left(\alpha_0^2 - \frac{\alpha_n^2}{\chi^2} \right) Z_n = 0 \quad .$$

This is the Bessel Equation and its general solution is

$$Z_n = aJ_{\alpha_n}(\alpha_0\chi) + bY_{\alpha_n}(\alpha_0\chi) \quad . \quad (34)$$

The boundary conditions are

$$Z_n(z=0) \equiv Z_n(\chi=1) = 0 \quad (35)$$

$$\frac{dZ_n}{dz}(z=H) \equiv \frac{dZ_n}{d\chi}(\chi=\chi_H) = 0 \quad . \quad (36)$$

The application of (35) and (36) to (34) results in two algebraic equations

$$aJ_{\alpha_n}(\alpha_0) + bY_{\alpha_n}(\alpha_0) = 0 \quad (37)$$

$$aJ'_{\alpha_n}(\alpha_0\chi_H) + bY'_{\alpha_n}(\alpha_0\chi_H) = 0 \quad . \quad (38)$$

As this linear system of algebraic equations is homogeneous, there is a nontrivial solution only if the corresponding Jacobian is zero, i.e.,

$$J_{\alpha_n}(\alpha_0)Y'_{\alpha_n}(\alpha_0\chi_H) - Y_{\alpha_n}(\alpha_0)J'_{\alpha_n}(\alpha_0\chi_H) = 0 \quad .$$

This characteristic equation must be solved in order to obtain the α_n 's, which are the scaled eigenvalues. After the α_n 's are evaluated, the κ_n 's can be determined using (33). It follows from the surface boundary condition, expressed in (37), that the specific solution, aside from a multiplicative constant, is

$$Z_n(z) \propto Y_{\alpha_n}(\alpha_0)J_{\alpha_n}(\alpha_0e^{-\beta z}) - J_{\alpha_n}(\alpha_0)Y_{\alpha_n}(\alpha_0e^{-\beta z}) \quad .$$

The constant of proportionality is given by normalization.

2. Negative Exponential Profile

The second profile considered is a downward refractive one. Here, sound speed decreases exponentially with depth and is given by

$$c(z) = c_0 e^{-\beta z} .$$

Thus, the Helmholtz Equation is

$$\frac{d^2 Z_n}{dz^2} + (\kappa_0^2 e^{\beta z} - \kappa_n^2) Z_n = 0 \quad (39)$$

where $\kappa_0 = \frac{\omega}{c_0}$.

With

$$\xi = e^{\beta z}$$

and α_0 and α_n given by (32) and (33) respectively, (39) can be recast as

$$\frac{1}{\xi} \frac{d}{d\xi} \left(\xi \frac{dZ_n}{d\xi} \right) + \left(\alpha_0^2 - \frac{\alpha_n^2}{\xi^2} \right) Z_n = 0 . \quad (40)$$

The general solution to (40) is

$$Z_n = a J_{\alpha_n}(\alpha_0 \xi) + b Y_{\alpha_n}(\alpha_0 \xi) .$$

Using the same analogy as in the previous case, we obtain as characteristic equation

$$J_{\alpha_n}(\alpha_0) Y'_{\alpha_n}(\alpha_0 \xi_H) - Y_{\alpha_n}(\alpha_0) J'_{\alpha_n}(\alpha_0 \xi_H) = 0 \quad (41)$$

and specific solution

$$Z_n(z) \propto Y_{\alpha_n}(\alpha_0) J_{\alpha_n}(\alpha_0 e^{\beta z}) - J_{\alpha_n}(\alpha_0) Y_{\alpha_n}(\alpha_0 e^{\beta z}) .$$

The κ_n 's can be found using (33) after solving (41) for the α_n 's.

3. Hyperbolic Profile

In this third case we assume that the sound speed has a minimum at $z = z_0$. The sound speed profile is

$$c(z') = c_0 \cosh(\beta z')$$

with

$$z' = z - z_0 .$$

The Helmholtz Equation to be solved is now

$$\frac{d^2 Z_n}{dz'^2} + \left[\left(\frac{\omega}{c_0} \right)^2 \frac{1}{\cosh^2(\beta z')} - \kappa_n^2 \right] Z_n = 0 . \quad (42)$$

With the following change of coordinates

$$\chi = \tanh(\beta z')$$

(42) becomes

$$\beta^2(1-\chi^2) \frac{d}{d\chi} \left[(1-\chi^2) \frac{dZ_n}{d\chi} \right] + [\kappa_0^2(1-\chi^2) - \kappa_n^2] Z_n = 0 . \quad (43)$$

After dividing (43) by $\beta^2(1-\chi^2)$ and using the definitions given in (32) and (33), (43) can be recast as

$$\frac{d}{d\chi} \left[(1-\chi^2) \frac{dZ_n}{d\chi} \right] + \left(\alpha_0^2 - \frac{\alpha_n^2}{1-\chi^2} \right) Z_n = 0 . \quad (44)$$

This is the Associated Legendre Equation. The general solution to (44) is

$$Z_n = aP_\nu^\mu(\chi) + bQ_\nu^\mu(\chi) ,$$

with

$$\mu = \alpha_n$$

and

$$\nu(\nu+1) = \alpha_0^2 .$$

The functions $P_\nu^\mu(\chi)$ and $Q_\nu^\mu(\chi)$ are the Associated Legendre Functions of the first and second kind of order μ and degree ν . Applying the boundary conditions we get the system of equations

$$aP_\nu^\mu(\chi_S) + bQ_\nu^\mu(\chi_S) = 0 \quad (45)$$

$$aP_v''(\chi_H) + bQ_v''(\chi_H) = 0$$

with

$$\chi_S = \tanh(-\beta z_0)$$

and

$$\chi_H = \tanh[\beta(H - z_0)] .$$

Thus, the corresponding characteristic equation is

$$P_v''(\chi_S)Q_v''(\chi_H) - Q_v''(\chi_S)P_v''(\chi_H) = 0 . \quad (46)$$

Solving (46) for μ gives the eigenvalues α_n 's and hence the horizontal wavenumbers κ_n 's. Using (45) the solution becomes

$$Z_n(z') \propto Q_v''(\chi_S)P_v''(\tanh \beta z') - P_v''(\chi_S)Q_v''(\tanh \beta z') .$$

B. ANALYTICAL EVALUATION OF WKB PHASE INTEGRALS AND DERIVATIVES

Now we use the WKB formulae to obtain the first order WKB solution for the three analytical sound speed profiles. The objective in this section is to evaluate analytically all the related WKB integrals and derivatives so that numerical errors can be eliminated in one of the error analysis. Horizontal wavenumbers computed using both the exact and approximate (i.e., WKB) characteristic equations will be compared in the next section. The evaluation of the horizontal wavenumbers is emphasized because they are the key parameters in normal mode computations.

1. Positive Exponential Profile

The vertical coordinate z is positive downward, the surface is at $z = 0$, the bottom at $z = H$ and the sound speed profile is

$$c(z) = c_0 e^{\beta z} .$$

With

$$\kappa_0 = \frac{\omega}{c_0}$$

the corresponding wavenumber profile is

$$\kappa = \kappa_0 e^{-\beta z} .$$

Let us first consider modes that have a turning point at $z = \hat{z}$. For $0 \leq z \leq \hat{z}$ (oscillatory region), κ_{zn} is given by

$$\kappa_{zn} = \kappa_0 \sqrt{e^{-2\beta z} - \gamma_n^2}$$

with

$$\gamma_n = \frac{\kappa_n}{\kappa_0} .$$

The spatial phase ϕ in this region is given by

$$\phi = \int_z^{\hat{z}} |\kappa_{zn}| dz . \quad (47)$$

With the change of coordinate

$$\chi = e^{-2\beta z}$$

(47) becomes

$$\phi = \frac{\kappa_0}{\beta} \left[\gamma_n \tan^{-1} \left(\sqrt{\frac{\chi - \gamma_n^2}{\gamma_n^2}} \right) - \sqrt{\chi - \gamma_n^2} \right]_{\chi(z)}^{\chi(\hat{z})} .$$

In the region $\hat{z} \leq z \leq H$ (exponential region), we must use

$$|\kappa_{zn}| = \sqrt{\kappa_n^2 - \kappa_0^2 e^{-2\beta z}} .$$

The spatial phase is now

$$\phi = \int_{\hat{z}}^z |\kappa_{zn}| dz ,$$

or, with

$$\xi = e^{-\beta z} ,$$

$$\phi = -\frac{\kappa_0}{\beta} \left[\sqrt{\gamma_n^2 - \xi^2} - \gamma_n \ln \left(\frac{\sqrt{\gamma_n^2 - \xi^2} + \gamma_n}{\xi} \right) \right]_{\xi(z)}^{\xi(\hat{z})}.$$

We must also compute

$$D = \left(\frac{1}{2|\kappa_{zn}|^2} \frac{d|\kappa_{zn}|}{dz} \right)_{z=H}$$

which can be equated as

$$D = \frac{\kappa_0^2 \beta}{2} \frac{e^{-\beta H}}{(\kappa_n^2 - \kappa_0^2 e^{-2\beta H})^{3/2}}.$$

Figure 1 shows a PR - TP mode in this upward refractive medium.

If the normal mode is PR-RB the phase is given by

$$\phi = \int_0^z |\kappa_{zn}| dz$$

or

$$\phi = \frac{\kappa_0}{\beta} \left[\gamma_n \tan^{-1} \left(\sqrt{\frac{\chi - \gamma_n^2}{\gamma_n^2}} \right) - \sqrt{\chi - \gamma_n^2} \right]_{\chi(0)}^{\chi(z)}$$

with

$$\chi(z) = e^{-2\beta z}$$

and

$$D = -\frac{\kappa_0^2 \beta}{2} \frac{e^{-2\beta H}}{(\kappa_0^2 e^{-2\beta H} - \kappa_n^2)^{3/2}}.$$

For each case we must also apply the respective characteristic equation.

2. Negative Exponential Profile

For this profile we have two types of normal modes: TP - RB and PR - RB.

The sound speed is

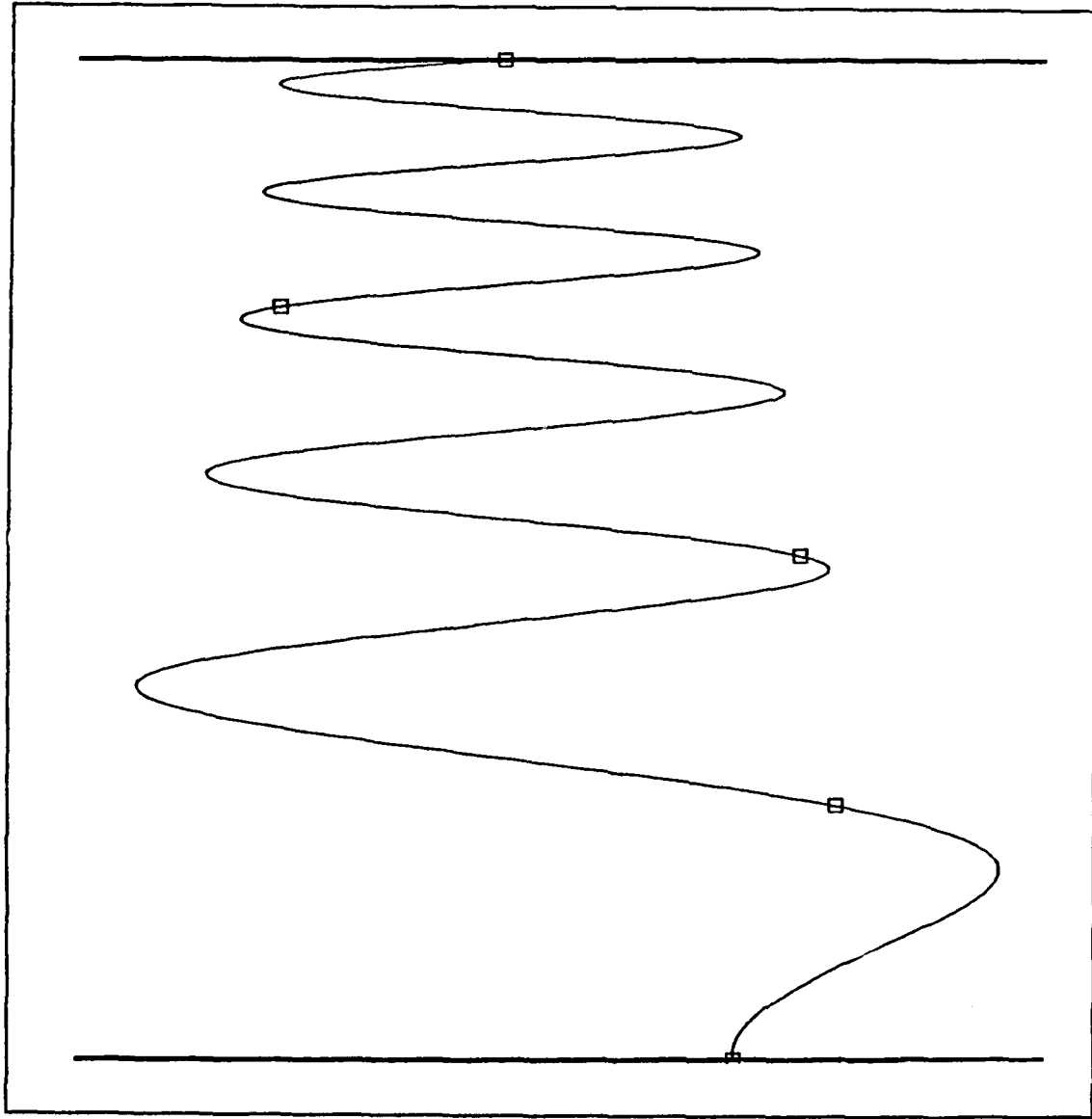


Figure 1. PR - TP Mode

$$c(z) = c_0 e^{-\beta z} .$$

Consequently, for a TP - RB normal mode and for $z \geq \hat{z}$ (oscillatory region) we have

$$|\kappa_{zn}| = \kappa_0 \sqrt{e^{2\beta z} - \gamma_n^2} .$$

So in this region the phase is

$$\phi = \frac{\kappa_0}{\beta} \left[\sqrt{\chi - \gamma_n^2} - \gamma_n \tan^{-1} \left(\sqrt{\frac{\chi - \gamma_n^2}{\gamma_n^2}} \right) \right]_{\chi(\hat{z})}^{\chi(z)}$$

with

$$\chi = e^{2\beta z}.$$

Also we have

$$D = \frac{\kappa_0^2 \beta}{2} \frac{e^{2\beta H}}{(\kappa_0^2 e^{2\beta H} - \kappa_n^2)^{3/2}}. \quad (48)$$

In the exponential region ($0 \leq z \leq \hat{z}$),

$$|\kappa_{zn}| = \kappa_0 \sqrt{\gamma_n^2 - e^{2\beta z}}$$

and thus the phase is

$$\phi = \frac{\kappa_0}{\beta} \left[\sqrt{\gamma_n^2 - \xi^2} - \gamma_n \ln \left| \frac{\sqrt{\gamma_n^2 - \xi^2} + \gamma_n}{\xi} \right| \right]_{\xi(z)}^{\xi(\hat{z})}$$

with

$$\xi = e^{\beta z}.$$

Figure 2 shows a TP - RB mode in such a downward refractive medium.

For a PR - RB normal mode we have

$$\phi = \frac{\kappa_0}{\beta} \left[\sqrt{\chi - \gamma_n^2} - \gamma_n \tan^{-1} \left(\sqrt{\frac{\chi - \gamma_n^2}{\gamma_n^2}} \right) \right]_{\chi(0)}^{\chi(z)}$$

and D is given by (48). Again, for each of the classes the respective characteristic equation must be used.

3. Hyperbolic Profile

We consider two types of normal modes: TP - TP and PR - RB. For the type TP - TP and in the oscillatory region ($\hat{z}'_1 \leq z \leq \hat{z}'_2$) the phase will be

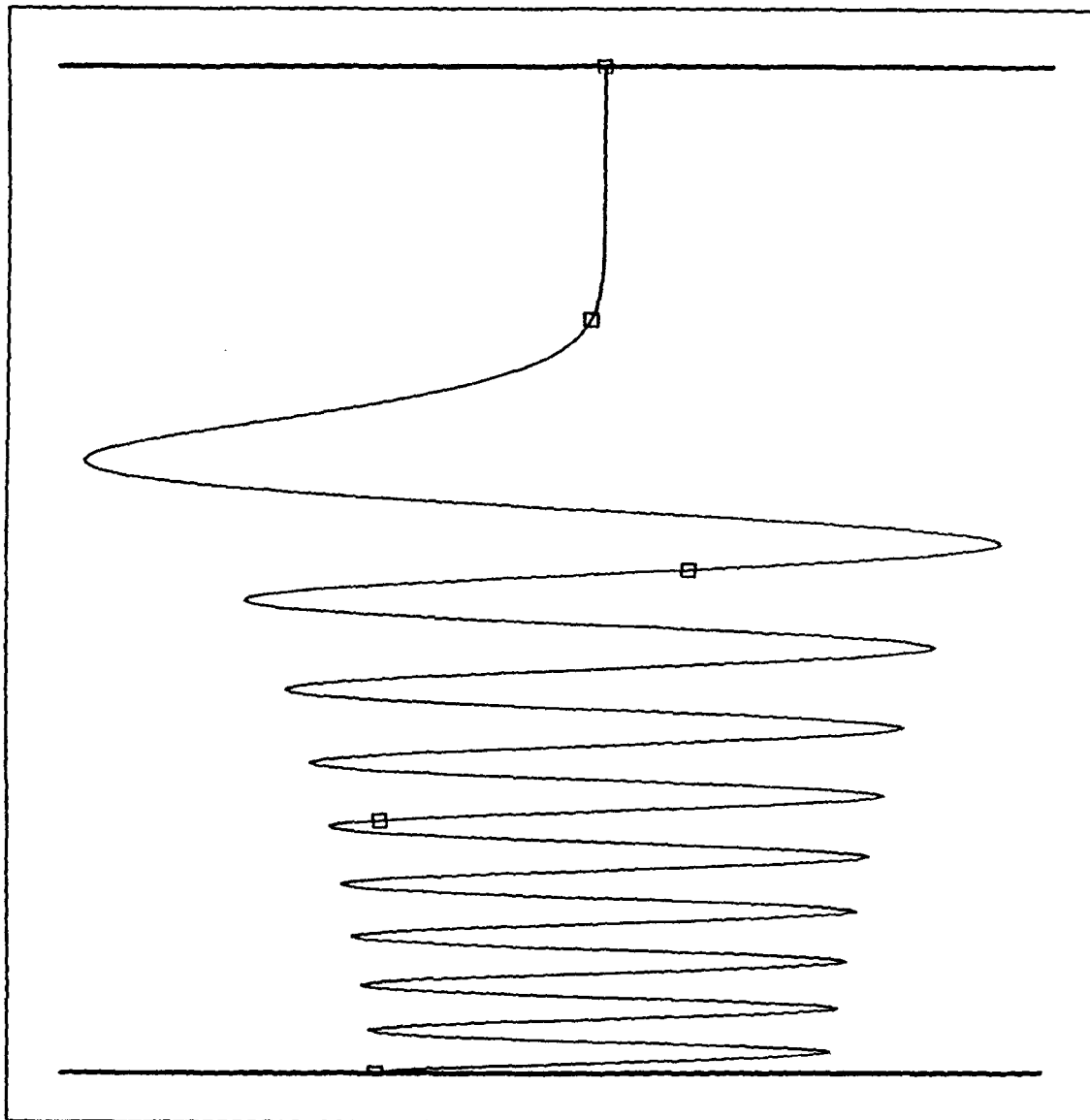


Figure 2. TP - RB Mode

$$\phi = \int_{z_2'}^{z'} |\kappa_{zn}| dz' \quad . \quad (49)$$

Using

$$\xi = \tanh(\beta z') \quad ,$$

$$\alpha_0 = \frac{\kappa_0}{\beta} ,$$

and

$$\eta_n^2 = 1 - \frac{\kappa_n^2}{\kappa_0^2} ,$$

(49) becomes

$$\phi = \alpha_0 \left[\sin^{-1} \left(\frac{\xi}{\eta_n} \right) - \sqrt{1 - \eta_n^2} \sin^{-1} \left(\frac{\xi \sqrt{1 - \eta_n^2}}{\eta_n \sqrt{1 - \xi^2}} \right) \right]_{\xi_1}^{\xi} .$$

For the exponential region near the bottom ($H \geq z' \geq \hat{z}'_2$) the phase is

$$\phi = \int_{z'}^{\hat{z}'_2} |\kappa_{zn}| dz'$$

or

$$\phi = \frac{\alpha_0}{2} \left[\ln \left| \frac{\xi - \sqrt{\xi^2 - \eta_n^2}}{\xi + \sqrt{\xi^2 - \eta_n^2}} \right| + \gamma_n \ln \left| \frac{1 + \xi}{1 - \xi} \frac{\gamma_n \sqrt{\xi^2 - \eta_n^2} - (1 - \xi) + \gamma_n^2}{\gamma_n \sqrt{\xi^2 - \eta_n^2} - (1 + \xi) + \gamma_n^2} \right| \right]_{\xi_2}^{\xi}$$

where

$$\gamma_n^2 = 1 - \eta_n^2 = \frac{\kappa_n^2}{\kappa_0^2} .$$

For this type of normal mode D is given by

$$D = \frac{\beta(1 - \xi_H^2) \kappa_0^2 \xi_H}{2[\kappa_n^2 - \kappa_0^2(1 - \xi_H^2)]^{3/2}} .$$

In the exponential region near the surface ($\hat{z}'_1 \geq z'$) the phase is

$$\phi = \frac{\alpha_0}{2} \left[\ln \left| \frac{\xi - \sqrt{\xi^2 - \eta_n^2}}{\xi + \sqrt{\xi^2 - \eta_n^2}} \right| + \gamma_n \ln \left| \frac{1 + \xi}{1 - \xi} \frac{\gamma_n \sqrt{\xi^2 - \eta_n^2} - (1 - \xi) + \gamma_n^2}{\gamma_n \sqrt{\xi^2 - \eta_n^2} - (1 + \xi) + \gamma_n^2} \right| \right]_{\xi}^{\hat{\xi}_1}$$

If the mode is PR - RB the phase will be

$$\phi = \alpha_0 \left[\sin^{-1} \left(\frac{\xi}{\eta_n} \right) - \sqrt{1 - \eta_n^2} \sin^{-1} \left(\frac{\xi \sqrt{1 - \eta_n^2}}{\eta_n \sqrt{1 - \xi^2}} \right) \right]_{\xi_S}^{\xi}$$

and D is given by

$$D = - \frac{\beta \kappa_0^2 \xi_H (1 - \xi_H^2)}{2 [\kappa_0^2 (1 - \xi_H^2) - \kappa_n^2]^{3/2}}$$

Figure 3 shows a TP - TP mode trapped by the refractive index.

C. COMPARISON OF RESULTS

1. Horizontal Wavenumber Error Analysis

The exact characteristic equations derived in section A for the three abstract profiles were solved using iterative procedures to obtain the benchmark κ_n 's. Similarly, the approximate WKB characteristic equations developed in the previous chapter were also solved for the three profiles with the use of the algebraic equations developed above. Very low frequencies were chosen for the comparison intentionally. This would give the WKB method a real test, since WKB is inherently a high-frequency approximation. For the exponential profiles, we used $\omega = 10 \text{ s}^{-1}$ or a frequency of 1.59 Hz. For the hyperbolic profile the frequency used was even lower, it was 0.23 Hz. Some of the computed horizontal wavenumbers (κ_n) are presented in Tables 1 through 5. The unit for κ_n is inverse meter (m^{-1}). The depth of the ocean is taken to be 10000 m.

In Tables 1 and 2 the exact and WKB results, as well as the absolute and relative errors, for the positive exponential profile are displayed. Tables 3 and 4 show the results for the negative exponential profile. In Table 5, the exact and approximate results for the hyperbolic profile are compared. At 0.23 Hz, mode 2 is TP - TP and mode 3 is PR - RB.

Overall, we can see that the absolute error (the absolute value of the WKB result minus the exact result) varies between 10^{-4} and 10^{-7} m^{-1} and the relative error (the

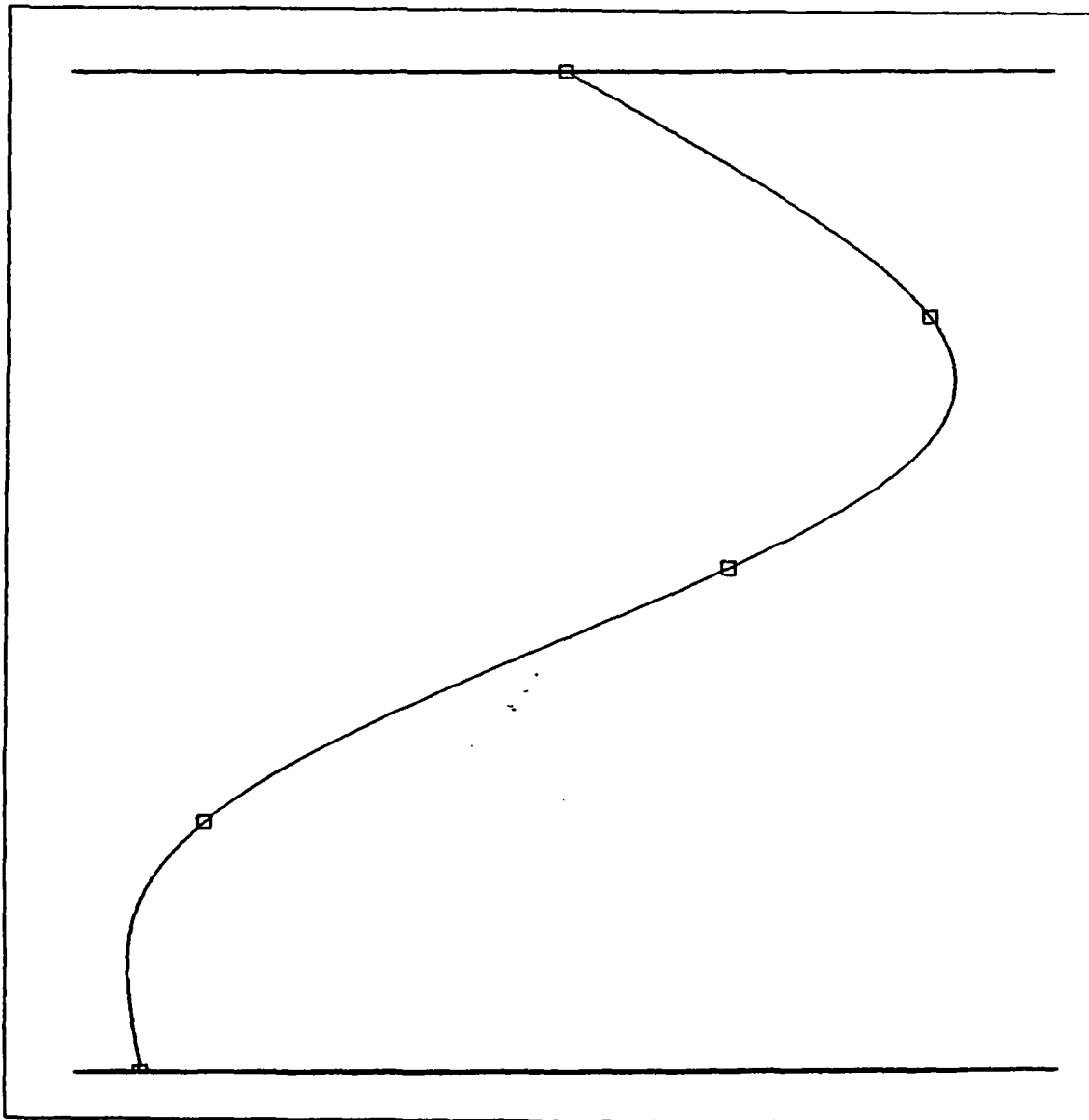


Figure 3. TP - TP Mode

absolute error divided by the exact value) varies between 10^{-2} and 10^{-5} . It is noted that for the modes with turning points not in close vicinity to the boundaries the absolute error usually stays below $10^{-5} m^{-1}$. The fact that the error increases when a turning point is close to a boundary is easily explained. The solutions in the critical regions are the less accurate because they use a linear approximation for κ_m^2 . So when they are used to match the boundary conditions the error increases.

Table 1. POSITIVE EXPONENTIAL PROFILE, PR - TP MODES

Mode #	Exact κ_n (m^{-1})	WKB κ_n (m^{-1})	Absolute Error (m^{-1})	Relative Error
5	$.43861 \times 10^{-2}$	$.43866 \times 10^{-2}$	5×10^{-7}	1.1×10^{-4}
6	$.40441 \times 10^{-2}$	$.40445 \times 10^{-2}$	4×10^{-7}	1.0×10^{-4}
7	$.37227 \times 10^{-2}$	$.37230 \times 10^{-2}$	3×10^{-7}	$.8 \times 10^{-4}$
8	$.34179 \times 10^{-2}$	$.34182 \times 10^{-2}$	3×10^{-7}	$.9 \times 10^{-4}$
9	$.31274 \times 10^{-2}$	$.31277 \times 10^{-2}$	3×10^{-7}	1×10^{-4}
10	$.28556 \times 10^{-2}$	$.28568 \times 10^{-2}$	1.2×10^{-6}	4.2×10^{-4}

Table 2. POSITIVE EXPONENTIAL PROFILE, PR - RB MODES

Mode #	Exact κ_n (m^{-1})	WKB κ_n (m^{-1})	Absolute Error (m^{-1})	Relative Error
12	$.23190 \times 10^{-2}$	$.23041 \times 10^{-2}$	1.5×10^{-5}	6.3×10^{-3}
13	$.18524 \times 10^{-2}$	$.18490 \times 10^{-2}$	3.4×10^{-6}	1.8×10^{-3}
14	$.10756 \times 10^{-2}$	$.10736 \times 10^{-2}$	2×10^{-6}	1.9×10^{-3}

Table 3. NEGATIVE EXPONENTIAL PROFILE, TP - RB MODES

Mode #	Exact κ_n (m^{-1})	WKB κ_n (m^{-1})	Absolute Error (m^{-1})	Relative Error
23	$.82307 \times 10^{-2}$	$.82308 \times 10^{-2}$	1×10^{-7}	1×10^{-5}
24	$.79463 \times 10^{-2}$	$.79464 \times 10^{-2}$	1×10^{-7}	1×10^{-5}
25	$.76664 \times 10^{-2}$	$.76665 \times 10^{-2}$	1×10^{-7}	1×10^{-5}
26	$.73903 \times 10^{-2}$	$.73904 \times 10^{-2}$	1×10^{-7}	1×10^{-5}
27	$.71158 \times 10^{-2}$	$.71155 \times 10^{-2}$	3×10^{-7}	4×10^{-5}

In general, for each type of mode the WKB approximation gets better as mode number increases. The only exception is when turning points are close to the boundaries. To see this, let us examine the results for the positive exponential profile (Tables 1 and 2). Starting from the lowest modes that have one turning point, the error decreases as mode number increases. At mode number 10, the accuracy of the WKB method de-

Table 4. NEGATIVE EXPONENTIAL PROFILE, PR - RB MODES

Mode #	Exact κ_n (m^{-1})	WKB κ_n (m^{-1})	Absolute Error (m^{-1})	Relative Error
29	$.65250 \times 10^{-2}$	$.65091 \times 10^{-2}$	1.6×10^{-5}	2.4×10^{-3}
30	$.61746 \times 10^{-2}$	$.61683 \times 10^{-2}$	1.6×10^{-5}	1.0×10^{-3}
31	$.57723 \times 10^{-2}$	$.57688 \times 10^{-2}$	3.5×10^{-6}	6.1×10^{-4}
32	$.53082 \times 10^{-2}$	$.53058 \times 10^{-2}$	2.4×10^{-6}	4.5×10^{-4}
33	$.47670 \times 10^{-2}$	$.47652 \times 10^{-2}$	1.8×10^{-6}	3.8×10^{-4}

Table 5. HYPERBOLIC PROFILE

Mode #	Exact κ_n (m^{-1})	WKB κ_n (m^{-1})	Absolute Error (m^{-1})	Relative Error
2	$.90114 \times 10^{-3}$	$.89881 \times 10^{-3}$	2.3×10^{-6}	2.2×10^{-3}
3	$.74139 \times 10^{-3}$	$.72953 \times 10^{-3}$	1.2×10^{-5}	1.6×10^{-2}

creases because the turning point comes too close to the bottom boundary. For mode 12 and higher a turning point does not exist and the oscillatory region is bounded by the physical boundaries. After the change of mode class the error starts to decrease again as mode number increases.

Errors in the κ_n 's for all cases are small enough that they do not significantly influence the vertically integrated phases ϕ because the maximum ocean depth is of the order of km's. In the horizontal direction the horizontal phase is approximately $\kappa_n r$ (this phase is exact when $c = c(z)$). The error in κ_n limits the range for which the use of WKB is accurate. If we want to keep the phase error below a few degrees, the tolerable error in κ_n is of the order of $10^{-5} m^{-1}$ for a range of 10 km, $10^{-6} m^{-1}$ for 100 km and $10^{-7} m^{-1}$ for 1000 km. All the κ_n 's associated with the modes that do not have interactions with the bottom boundary, as calculated from the WKB method, have errors less than $10^{-6} m^{-1}$, implying that the method is good to at least 100 km at 1 Hz. For higher frequencies the results would be much better.

2. Errors In The Interference Distances

The acoustic pressure square at far field can be written as (assuming no range dependence)

$$[p(r,z)]^2 = \frac{1}{r} \sum_{n=1}^{\infty} A_n^2 Z_n^2(z_0) Z_n^2(z) + \frac{1}{r} \sum_{n=1}^{\infty} \sum_{\substack{m=1 \\ m \neq n}}^{\infty} A_n A_m Z_n(z_0) Z_m(z_0) Z_n(z) Z_m(z) \cos[(\kappa_m - \kappa_n)r]$$

where the A_n 's are constants and the acoustic source is at $z = z_0$ and $r = 0$ (Clay and Medwin, 1977). We can see that the interference terms are functions of the differences of horizontal wavenumbers. The interference distance (or interference wavelength) defined by

$$\Lambda_{nm} = \left| \frac{2\pi}{\kappa_m - \kappa_n} \right|$$

is therefore an important parameter for transmission loss calculation (Chiu and Ehret, 1990). In general, dominant interferences are between adjacent modes (Chiu and Ehret, 1990). So let us see what is the size of the errors in $\Delta\kappa_n = |\kappa_{n-1} - \kappa_n|$ computed using the WKB approximation. In Tables 6 and 7 we display the exact and WKB $\Delta\kappa_n$'s, as well as the absolute errors. As expected, we can see that the errors in $\Delta\kappa_n$ vary in a similar way as in κ_n and are slightly smaller.

Table 6. POSITIVE EXPONENTIAL PROFILE, PR - TP MODES

n	Exact $\Delta\kappa_n$ (m^{-1})	WKB $\Delta\kappa_n$ (m^{-1})	Absolute Error (m^{-1})
5	$.3420 \times 10^{-3}$	$.3421 \times 10^{-3}$	1×10^{-7}
6	$.3214 \times 10^{-3}$	$.3215 \times 10^{-3}$	1×10^{-7}
7	$.3048 \times 10^{-3}$	$.3048 \times 10^{-3}$	~ 0
8	$.2905 \times 10^{-3}$	$.2905 \times 10^{-3}$	~ 0
9	$.2718 \times 10^{-3}$	$.2709 \times 10^{-3}$	9×10^{-7}

3. General Numerical Method

The WKB results in the previous section were obtained using analytical means rather than numerical methods. The reason for that was we wanted to see how accurate the WKB approximation is regardless of the numerical methods used to evaluate integrals and derivatives. As we see, absolute errors in the order of $10^{-7} m^{-1}$ for the κ_n 's are achieved at 1 Hz. This means that the WKB solution is very accurate, especially because we used very low frequencies.

Table 7. POSITIVE EXPONENTIAL PROFILE, PR - RB MODES

n	Exact $\Delta\kappa_n$ (m^{-1})	WKB $\Delta\kappa_n$ (m^{-1})	Absolute Error (m^{-1})
12	$.4666 \times 10^{-3}$	$.4551 \times 10^{-3}$	1.15×10^{-5}
13	$.7768 \times 10^{-3}$	$.7754 \times 10^{-3}$	1.4×10^{-6}

For an arbitrary profile all the integrations and differentiations must be done numerically. It is expected that the errors will increase due to numerical noise. The Fortran program WKBGEN (Appendix C) developed in this thesis can be applied to an arbitrary profile. For each mode it finds class, horizontal wavenumber and depths of the turning points. This program was also applied to the three abstract profiles. Some numerical results for the κ_n 's are presented in Tables 8 through 11.

Tables 8 and 9 show the exact and numerical WKB results and the respective absolute errors for the positive exponential profile. Tables 10 and 11 show the corresponding results for the negative exponential profile.

Table 8. POSITIVE EXPONENTIAL PROFILE, PR - TP MODES

Mode #	Exact κ_n (m^{-1})	WKB κ_n (m^{-1})	Absolute Error (m^{-1})
5	$.43861 \times 10^{-2}$	$.43874 \times 10^{-2}$	1.3×10^{-6}
6	$.40441 \times 10^{-2}$	$.40454 \times 10^{-2}$	1.3×10^{-6}
7	$.37227 \times 10^{-2}$	$.37234 \times 10^{-2}$	7×10^{-7}
8	$.34179 \times 10^{-2}$	$.34184 \times 10^{-2}$	5×10^{-7}
9	$.31274 \times 10^{-2}$	$.31284 \times 10^{-2}$	1×10^{-6}
10	$.28556 \times 10^{-2}$	$.28574 \times 10^{-2}$	1.8×10^{-6}

As we can see, the errors in the κ_n 's computed using the numerical method are slightly larger than the previous results (Tables 1 through 4) but are approximately in the same order of magnitude.

Table 9. POSITIVE EXPONENTIAL PROFILE, PR - RB MODES

Mode #	Exact $\kappa_n (m^{-1})$	WKB $\kappa_n (m^{-1})$	Absolute Error (m^{-1})
12	$.23190 \times 10^{-2}$	$.23044 \times 10^{-2}$	1.5×10^{-5}
13	$.18524 \times 10^{-2}$	$.18494 \times 10^{-2}$	3.0×10^{-6}
14	$.10756 \times 10^{-2}$	$.10744 \times 10^{-2}$	1.2×10^{-6}

Table 10. NEGATIVE EXPONENTIAL PROFILE, TP - RB MODES

Mode #	Exact $\kappa_n (m^{-1})$	WKB $\kappa_n (m^{-1})$	Absolute Error (m^{-1})
23	$.82307 \times 10^{-2}$	$.82309 \times 10^{-2}$	2×10^{-7}
24	$.79463 \times 10^{-2}$	$.79469 \times 10^{-2}$	6×10^{-7}
25	$.76664 \times 10^{-2}$	$.76669 \times 10^{-2}$	5×10^{-7}
26	$.73903 \times 10^{-2}$	$.73909 \times 10^{-2}$	6×10^{-7}
27	$.71158 \times 10^{-2}$	$.71159 \times 10^{-2}$	1×10^{-7}

Table 11. NEGATIVE EXPONENTIAL PROFILE, PR - RB MODES

Mode #	Exact $\kappa_n (m^{-1})$	WKB $\kappa_n (m^{-1})$	Absolute Error (m^{-1})
30	$.61746 \times 10^{-2}$	$.61689 \times 10^{-2}$	5.7×10^{-6}
31	$.57723 \times 10^{-2}$	$.57689 \times 10^{-2}$	3.4×10^{-6}
32	$.53082 \times 10^{-2}$	$.53059 \times 10^{-2}$	2.3×10^{-6}
33	$.47670 \times 10^{-2}$	$.47649 \times 10^{-2}$	2.1×10^{-6}

IV. CONCLUSIONS AND RECOMMENDATIONS

The WKB approximations of acoustic normal modes seem to give results accurate enough to be of practical use. Although WKB is inherently a high frequency approximation, meaning that it works better for higher frequency, the results from our tests show that, even for frequencies around one Hertz, this technique has an appreciable accuracy.

When applying the WKB algorithm for arbitrary sound speed profiles the determination of the class of each normal mode must be done carefully. Each class has different formulae. There are a total of four classes in a single duct or channel environment.

A small weakness of the method is that the error in the WKB solution increases when a turning point is very close to a boundary. However, the corresponding errors are still very small for the exponential and hyperbolic profiles used in this study.

The exact analytical solutions to the Helmholtz Equation can also be used for comparison to any other methods. These exact solutions are subject to pressure release surface and rigid bottom boundary conditions. Exact solutions can also be found for any boundary conditions. Specifically, we can maintain the pressure release surface boundary condition, which is a good assumption, and use a non-rigid bottom boundary condition.

Some difficulties were found when working with Bessel and Associated Legendre Functions. The IMSL subroutines used for Bessel Function evaluation cannot handle some orders and values of the argument. With respect to the evaluation of Associated Legendre Functions, subroutines are not available in the IMSL libraries. Some Fortran programs were coded to compute them. These programs also work only for certain ranges of order, degree and arguments of the functions. Further programming work concerning these transcendental functions is recommended.

WKB formulae for modes trapped in the water column over a non-rigid bottom were derived in Appendix B although they are not implemented for this analysis. A general mathematical expression for boundary conditions for normal modes is also presented in Appendix B. The use of this mathematical expression is not a trivial matter because the expression depends on the density and the sound speed profile of the sediment. Further studies on using WKB algorithms for arbitrary bottom boundary conditions are recommended.

In this thesis only single duct/channel environments have been considered. Essentially, we have ignored double duct/channel problems. However, the WKB approximation method has been applied to other nonacoustic but equivalent double duct/channel problems (for example, transmission of electromagnetic waves through potential barriers) with success (Bender and Orszag, 1978).

In conclusion, the WKB method allows for accurate and fast computation of normal modes and their eigenvalues. In addition, it allows for storage of the results in terms of only a few parameters for each mode.

APPENDIX A. FIRST ORDER WKB THEORY

With

$$d\phi = |\kappa_{zn}| dz$$

the Helmholtz Equation becomes

$$\frac{d^2 Z_n}{d\phi^2} + \frac{1}{|\kappa_{zn}|} \frac{d|\kappa_{zn}|}{d\phi} \frac{dZ_n}{d\phi} + Z_n = 0 \quad (A.1)$$

This equation has some similarities with a Bessel Equation. Let us try a solution in the form

$$Z_n \propto \sqrt{\frac{\phi}{|\kappa_{zn}|}} F(\phi).$$

Substituting this trial solution form in (A.1) we get

$$\frac{d^2 F}{d\phi^2} + \frac{1}{\phi} \frac{dF}{d\phi} + \left[1 + r(z) - \frac{(1/2)^2}{\phi^2} \right] F = 0 \quad (A.2)$$

with

$$r(z) = 1 + \frac{3}{4} \frac{1}{|\kappa_{zn}|^4} \left(\frac{d|\kappa_{zn}|}{dz} \right)^2 - \frac{1}{2} \frac{1}{|\kappa_{zn}|^3} \frac{d^2 |\kappa_{zn}|}{dz^2}.$$

If $r(z)$ is negligible, i.e., $|r(z)| \ll 1$, (A.2) can be approximated as

$$\frac{d^2 F}{d\phi^2} + \frac{1}{\phi} \frac{dF}{d\phi} + \left[1 - \frac{(1/2)^2}{\phi^2} \right] F = 0 \quad (A.3)$$

which is a Bessel Equation.

The general solution to (A.3), for $\kappa_{zn}^2 > 0$, is

$$F(\phi) = a' J_{1/2}(\phi) + b' Y_{1/2}(\phi) \quad (A.4)$$

where $J_{1/2}$ and $Y_{1/2}$ are the order 1/2 Bessel Functions of the 1st and 2nd kind, respectively.

But since

$$J_{1/2} \propto \frac{\sin x}{\sqrt{x}}$$

$$Y_{1/2} \propto \frac{\cos x}{\sqrt{x}}$$

(A.4) becomes

$$F(\phi) = a \frac{\sin \phi}{\sqrt{\phi}} + b \frac{\cos \phi}{\sqrt{\phi}}$$

and thus

$$Z_n(z) = \frac{a \sin \phi + b \cos \phi}{\sqrt{\kappa_{zn}}} .$$

If $\kappa_{zn}^2 < 0$, instead of (A.3) we would get the Modified Bessel Equation whose general solution is given by

$$F(\phi) = a' K_{1/2}(\phi) + b' I_{1/2}(\phi)$$

where $K_{1/2}$ and $I_{1/2}$ are the Modified Bessel Functions. Since

$$K_{1/2}(\phi) \propto \frac{e^{-\phi}}{\sqrt{\phi}}$$

$$I_{1/2}(\phi) \propto \frac{e^{\phi}}{\sqrt{\phi}}$$

we now have

$$F(\phi) = \frac{ae^{-\phi} + be^{\phi}}{\sqrt{\phi}}$$

and thus

$$Z_n(z) = \frac{ae^{-\phi} + be^{\phi}}{\sqrt{|\kappa_{zn}|}} .$$

Let us assume that there is a turning point at $z=0$, $\kappa_{zn}^2 > 0$ for $z > 0$, $\kappa_{zn}^2 < 0$ for $z < 0$ and near the turning point $\kappa_{zn}^2 = \gamma z$. So, close to the turning point we have

$$\phi = \int_0^z |\kappa_{zn}| dz = s \frac{2}{3} \gamma^{1/2} |z|^{3/2}$$

with $s = z/|z|$, and after some algebra,

$$\frac{1}{|\kappa_{zn}|} \frac{d|\kappa_{zn}|}{d\phi} = \frac{1}{3\phi}$$

Using this in (A.1) we get

$$\frac{d^2 Z_n}{d\phi^2} + \frac{1}{3\phi} \frac{dZ_n}{d\phi} + Z_n = 0 \quad (A.5)$$

Let us now look for a solution near the turning point in the form

$$Z_n \propto \left(\frac{3}{2} \phi \right)^{1/3} F(\phi).$$

Substituting this solution form in (A.5) we get

$$\frac{d^2 F}{d\phi^2} + \frac{1}{\phi} \frac{dF}{d\phi} + \left[1 - \frac{(1/3)^2}{\phi^2} \right] F = 0$$

whose general solution is

$$F(\phi) = c_1 B_{-1/3}(\phi) + c_2 B_{1/3}(\phi)$$

where B represents Bessel Functions. For $\kappa_{zn}^2 > 0$ they are $J_{-1/3}$ and $J_{1/3}$. For $\kappa_{zn}^2 < 0$ they are $I_{-1/3}$ and $I_{1/3}$. Relating Z_n with F we obtain

$$Z_n = \left(\frac{3}{2} \phi \right)^{1/3} [c_1 B_{-1/3}(\phi) + c_2 B_{1/3}(\phi)]$$

or

$$Z_n = \sqrt{\gamma^{1/3} |z|} \left[c_1 B_{-1/3} \left(\pm \frac{2}{3} \gamma^{1/2} |z|^{3/2} \right) + c_2 B_{1/3} \left(\pm \frac{2}{3} \gamma^{1/2} |z|^{3/2} \right) \right] \quad (A.6)$$

where the plus sign is for $\kappa_{zn}^2 < 0$ and the minus sign for $\kappa_{zn}^2 > 0$. A way to avoid the inconvenience of sign switching is to use Airy Functions which are related to $B_{\pm 1,3}$ (see Chapter III, Section A).

APPENDIX B. GENERAL BOUNDARY CONDITIONS

A. GENERAL FORMULA

Until now we have assumed that the boundary conditions are pressure release at the surface and rigid bottom. The first one is a good assumption but the second one can be far away from reality. Let us now present a general bottom condition formula for normal modes that depends on the bottom characteristics.

The acoustic pressure due to the n^{th} mode is

$$p_n = Z_n(z) R_n(r, \theta) e^{i\omega t} \quad (B.1)$$

The vertical component of the momentum equation relating p_n to the vertical particle velocity u_{Nn} in the n^{th} mode is

$$\rho_1 \frac{\partial u_{Nn}}{\partial t} = - \frac{\partial p_n}{\partial z} \quad (B.2)$$

where ρ_1 is the water density and the bottom is assumed to be flat. Using (B.1) in (B.2) we get

$$u_{Nn} = \frac{i}{\rho_1 \omega} \frac{dZ_n}{dz} R_n e^{i\omega t} \quad (B.3)$$

At the bottom boundary, the requirement is that both p_n and u_{Nn} are continuous across the water-sediment interface. In other words, the normal acoustic impedance across the interface is continuous. The normal acoustic impedance associated with the n^{th} mode is

$$\tilde{z}_{Nn} = \frac{p_n}{u_{Nn}} \quad (B.4)$$

By using (B.1) and (B.3) in (B.4) one can obtain as a general condition

$$\left(\frac{dZ_n}{dz} + i \frac{\rho_1 \omega}{\tilde{z}_{Nn}} Z_n \right)_{z=H} = 0 \quad (B.5)$$

if \tilde{z}_{Nn} at the water-sediment interface is known from the sediment properties.

Let us use a local plane wave approximation of the normal mode near $z = H$ in the water column, i.e.,

$$Z_n(z) = A_n [e^{-i\kappa_{Hn}(z-H)} + R e^{i\kappa_{Hn}(z-H)}]$$

where A_n is a constant, R is the complex plane wave reflection coefficient and κ_{Hn} is the vertical wavenumber in water computed at the boundary (Clay and Medwin, 1977). With this plane wave approximation, one can easily show that (Kinsler et al., 1982)

$$\tilde{z}_{Nn} = \frac{\rho_2 c_{2b}}{\sqrt{1 - \left(\frac{c_{2b}}{c_{1b}}\right)^2 \left(\frac{c_{2b}}{\omega}\right)^2 \kappa_n^2}} \quad (B.6)$$

where the index 1 refers to water, 2 refers to sediment and b refers to the value at the boundary. R is also known as the Rayleigh Reflection Coefficient which can be equated as

$$R = \left(\frac{\frac{\rho_2}{\rho_1} - \frac{\kappa_{2zn}}{\kappa_{zn}}}{\frac{\rho_2}{\rho_1} + \frac{\kappa_{2zn}}{\kappa_{zn}}} \right)_{z=H}$$

where κ_{2zn} is the vertical wavenumber in the sediment layer and is given by

$$\kappa_{2zn}^2 = \frac{\omega^2}{c_2^2} - \kappa_n^2,$$

and κ_n is the usual vertical wavenumber in the water column (Kinsler et al., 1982).

Substituting (B.6) in (B.5) we can rewrite (B.5) as

$$\left(\frac{dZ_n}{dz} + i \frac{\rho_1}{\rho_2} \kappa_{2zn} Z_n \right)_{z=H} = 0. \quad (B.7)$$

A more intuitive form for (B.7) is

$$\left(\frac{dZ_n}{dz} + i \frac{1-R}{1+R} \kappa_{Hn} Z_n \right)_{z=H} = 0. \quad (B.8)$$

As expected, for a rigid boundary ($R = 1$).

$$\left(\frac{dZ_n}{dz} \right)_{z=H} = 0$$

and, for a pressure release boundary ($R = -1$),

$$(Z_n)_{z=H} = 0 .$$

B. TRAPPED MODES IN THE WATER COLUMN

We will consider only modes that are trapped in the water layer in this WKB formulation. This means that κ_{zn} is purely imaginary or

$$\kappa_{zn} = i\beta_n$$

with β_n real and defined by

$$\beta_n = -\sqrt{\kappa_n^2 - \frac{\omega^2}{c_2^2}} . \quad (B.9)$$

Substituting (B.9) in (B.7) we get

$$\left(\frac{dZ_n}{dz} - \frac{\rho_1}{\rho_2} \beta_n Z_n \right)_{z=H} = 0 . \quad (B.10)$$

Since (B.7) is a general boundary condition, (B.10) is also general but is only applicable to modes trapped in the water column. We will apply (B.10) to each class of normal modes in the water column.

1. Class I

As usual we assume that there is a turning point at $z = \hat{z}$ with $0 < \hat{z} < H$. In the exponential region ($\hat{z} < z < H$) the solution is

$$Z_n = \frac{1}{\sqrt{|\kappa_{zn}|}} \cosh(\phi - \phi_b) \quad (B.11)$$

with

$$\phi = \int_{\hat{z}}^z |\kappa_{zn}| dz$$

and

$$|\kappa_{zn}| = \sqrt{\kappa_n^2 - \frac{\omega^2}{c_1^2}} .$$

As (B.11) must satisfy (B.10), ϕ_δ must be

$$\phi_\delta = \int_{\hat{z}}^H |\kappa_{zn}| dz - \tanh^{-1} \left(\frac{1}{2|\kappa_{zn}|^2} \frac{d|\kappa_{zn}|}{dz} + \frac{\rho_1}{\rho_2} \frac{\beta_n}{|\kappa_{zn}|} \right)_{z=H} \quad (B.12)$$

with β_n given by (B.9). The only difference relative to the rigid bottom case is expression for ϕ_δ . All the other formulae remain unchanged.

2. Class II

In the oscillatory region, $\hat{z} < z < H$, the solution is

$$Z_n = \frac{e^{\phi_s}}{\sqrt{\kappa_{zn}}} \sin\left(\phi + \frac{\pi}{4}\right) - \frac{e^{-\phi_s}}{2\sqrt{\kappa_{zn}}} \cos\left(\phi + \frac{\pi}{4}\right) \quad (B.13)$$

with

$$\phi = \int_{\hat{z}}^z |\kappa_{zn}| dz$$

and

$$\phi_s = \int_0^{\hat{z}} |\kappa_{zn}| dz .$$

(B.13) must satisfy (B.10), implying that

$$\sin \left\{ \phi_H + \frac{\pi}{4} + \tan^{-1} \left[\frac{e^{\phi_s} + \frac{D+E}{2} e^{-\phi_s}}{\frac{e^{-\phi_s}}{2} - (D+E)e^{\phi_s}} \right] \right\} = 0 \quad (B.14)$$

where D is defined in Chapter II, Equation (22),

$$\phi_H = \int_{\hat{z}}^H \kappa_{zn} dz$$

and

$$E = \left(\frac{\rho_1}{\rho_2} \frac{\beta_n}{\kappa_{zn}} \right)_{z=H} . \quad (B.15)$$

Therefore, the characteristic equation following from (B.14) is

$$\int_2^H \kappa_{zn} dz = \left(n - \frac{1}{4} \right) \pi - \alpha$$

for $D < 0$, and

$$\int_2^H \kappa_{zn} dz = \left(n - \frac{5}{4} \right) \pi - \alpha$$

for $D > 0$, where

$$\alpha = \tan^{-1} \left[\frac{e^{\phi_s} + \frac{D+E}{2} e^{-\phi_s}}{\frac{e^{-\phi_s}}{2} - (D+E)e^{\phi_s}} \right] .$$

All the other formulae are identical to the rigid bottom case.

3. Class III

For this class the only difference relative to the rigid bottom case is that ϕ_s must now be computed with (B.12).

4. Class IV

The solution over the entire ocean depth is

$$Z_n = \frac{1}{\sqrt{\kappa_{zn}}} \sin \phi$$

with

$$\phi = \int_0^z |\kappa_{zn}| dz .$$

To satisfy (B.10) we require

$$\int_0^H \kappa_{zn} dz = n\pi - \tan^{-1} \left(\frac{1}{D+E} \right)$$

for $D > 0$, and

$$\int_0^H \kappa_{zn} dz = n\pi + \tan^{-1} \left(\frac{1}{D+E} \right)$$

for $D < 0$, with E given by (B.15). This is now the Class IV mode characteristic equation.

APPENDIX C. FORTRAN PROGRAM WKBGEN

A. PROGRAM DESCRIPTION

The program WKBGEN is formed by a main program and several subprograms. The main program evaluates the minimum sound speed and then controls the subprograms. The inputs must be given in the PARAMETER statement. The inputs include the ocean depth (H), acoustic frequency (F), the wavenumber increment used in the κ_n search (DK), first mode (NMI) and last one (NMF) to be computed. The units in this program are those of the MKS system. The input sound speed profile is specified using the subprogram FUNCTION C(Z). SUBROUTINE TYPE evaluates the class of each mode. SUBROUTINE CHARAC controls the search for κ_n and the turning points. The appropriate characteristic equation is given by FUNCTION EQCHAR and the turning points are evaluated by SUBROUTINE ZTURN. The auxiliary subprograms FUNCTION PHASE, FUNCTION FKZ2 and FUNCTION FKZ evaluate respectively the phase integral, κ_m^2 and $|\kappa_m|$. The Airy Functions are computed by the FUNCTION's AI(Z) and BI(Z) and their derivatives by FUNCTION's DAI(Z) and DBI(Z). These four subprograms use the SUBROUTINE's MMBSJR and MMBSIR in the IMSL libraries to evaluate the Bessel and Modified Bessel Functions, respectively.

As output, the mode numbers and the respective eigenvalues are printed on the screen. These results, as well as the depths of the turning points, are also written in a file whose name is specified in the CALL EXCMS statement at the beginning of the main program.

The numerical method used to solve for the characteristic equation and to find the turning depths is the simple but safe Bisection Method (Gerald and Wheatley, 1989). The method to compute integrals is the Trapezoidal Rule (Gerald and Wheatley, 1989). Derivatives are evaluated by forward or backward finite differences (Gerald and Wheatley, 1989).

B. PROGRAM LISTING

PROGRAM WKBGEN

```
C
C
C*****
C
C    MAIN PROGRAM
C
C
```

```

IMPLICIT REAL*8 (A-H,O-Z)
PARAMETER (H=      ,F=      ,DK=      ,NMI=      ,NMF=      )
C
C
C
CALL EXCMS('FILEDEF 1 DISK WKBGEN DATA A')
OM=8.DO*DATAN(1.DO)*F
ZEX=DMOD(H,10.DO)
C
C
C
CS=C(0)
CB=C(H)
C
C
C
CM=99999.DO
DO Z=0.DO,H-ZEX,10.DO
    CM=DMIN1(CM,C(Z))
END DO
CM=DMIN1(CM,C(H))
C
C
C
XK0=OM/CM
XKL=XK0
C
C
C
DO N=NMI,NMF
C
DO XKI=XKL,0,DK
C
XKF=XKI+DK
CNI=OM/XKI
CNF=OM/XKF
CALL TYPE(CNI,CS,CB,NTYPE)
CALL ZTURN(CNI,H,ZEX,NTYPE,ZI1,ZI2)
CALL ZTURN(CNF,H,ZEX,NTYPE,ZF1,ZF2)
CALL CHARAC(OM,H,ZEX,N,XKI,XKF,NTYPE,ZI1,ZI2,ZF1,ZF2,NSOL,XKSOL,
$          ZT1,ZT2)
IF (NSOL.EQ.1) GO TO 100
C
END DO
C
100 PRINT*,N,XKSOL
C
IF (NTYPE.EQ.1.OR.NTYPE.EQ.2) THEN
    WRITE (1,*) N,NTYPE,XKSOL,ZT1
ELSE IF (NTYPE.EQ.3) THEN
    WRITE (1,*) N,NTYPE,XKSOL,ZT1,ZT2
ELSE
    WRITE (1,*) N,NTYPE,XKSOL
END IF
C
XKL=XKSOL

```

```

END DO
STOP
END
C
C
C
C*****
C
C
C
C
SUBROUTINE TYPE(CN,CS,CB,NTYPE)
REAL*8 CN,CS,CB
C
IF (CN.GT.CS.AND.CN.LT.CB) THEN
  NTYPE=1
ELSE IF (CN.LT.CS.AND.CN.GT.CB) THEN
  NTYPE=2
ELSE IF (CN.LT.CS.AND.CN.LT.CB) THEN
  NTYPE=3
ELSE
  NTYPE=4
END IF
C
RETURN
END
C
C
C
C*****
C
C
C
SUBROUTINE CHARAC(OM,H,ZEX,NM,XI,XF,NT,ZI1,ZI2,ZF1,ZF2,NSOL,XSOL,
$              Z21,Z22)
IMPLICIT REAL*8 (A-H,O-Z)
XSOL=9999.D0
NSOL=1
FI=EQCHAR(NM,NT,H,OM,XI,ZI1,ZI2)
FF=EQCHAR(NM,NT,H,OM,XF,ZF1,ZF2)
IF ((FI*FF).GT.0.D0) THEN
  NSOL=0
  GO TO 100
ELSE IF (FI.EQ.0.D0) THEN
  XSOL=XI
  GO TO 500
ELSE IF (FF.EQ.0.D0) THEN
  XSOL=XF
  GO TO 500
ELSE
  CONTINUE
END IF
DO 200 N=1,500
XM2=(XF+XI)/2.D0
IF(N.EQ.1) GO TO 50
IF ((XM2-XM1).EQ.0.D0) THEN
  XSOL=XM2

```

```

        GO TO 500
    END IF
50  XM1=XM2
    CN2=OM/XM2
    CALL ZTURN(CN2,H,ZEX,NT,Z21,Z22)
    F2=EQCHAR(NM,NT,H,OM,X2,Z21,Z22)
    IF ((F2*FF).LT.0.DO) THEN
        XI=XM2
    ELSE
        XF=XM2
        FF=F2
    END IF
200 CONTINUE
100 CONTINUE
500 CONTINUE
    RETURN
    END

C
C
C
C*****
C
C
C
C
SUBROUTINE ZTURN(CN,H,ZEX,NT,ZT1,ZT2)
    IMPLICIT REAL*8 (A-H,O-Z)
    REAL*8 NM
    ZT1=99999.DO
    ZT2=99999.DO
    DO 100 D= 0.DO,H,10.DO
        XF=D+10.DO
        XI=D
        FI=C(XI)-CN
        FF=C(XF)-CN
        IF ((FI*FF).GT.0.DO) THEN
            GO TO 100
        ELSE IF (FI.EQ.0.DO) THEN
            XSOL=XI
            GO TO 500
        ELSE IF (FF.EQ.0.DO) THEN
            XSOL=XF
            GO TO 500
        ELSE
            CONTINUE
        END IF
    DO 200 N=1,500
        XM2=(XF+XI)/2.DO
        IF(N.EQ.1) GO TO 50
        IF ((XM2-XM1).EQ.0.DO) THEN
            XSOL=XM2
            GO TO 500
        END IF
50  XM1=XM2
        F2=C(XM2)-CN
        IF ((F2*FF).LT.0.DO) THEN
            XI=XM2

```



```

ELSE
  XF=XM2
  FF=F2
END IF
200 CONTINUE
100 CONTINUE
500 CONTINUE
ZT1=XSOL
IF (NT.EQ.3) THEN
  DO 110 D= H,0.D0,-10.D0
  XF=D-10.D0
  XI=D
  FI=C(XI)-CN
  FF=C(XF)-CN
  IF ((FI*FF).GT.0.D0) THEN
    GO TO 110
  ELSE IF (FI.EQ.0.D0) THEN
    XSOL=XI
    GO TO 510
  ELSE IF (FF.EQ.0.D0) THEN
    XSOL=XF
    GO TO 510
  ELSE
    CONTINUE
  END IF
  DO 210 N=1,510
  XM2=(XF+XI)/2.D0
  IF(N.EQ.1) GO TO 51
  IF ((XM2-XM1).EQ.0.D0) THEN
    XSOL=XM2
    GO TO 510
  END IF
51  XM1=XM2
  F2=C(XM2)-CN
  IF ((F2*FF).LT.0.D0) THEN
    XI=XM2
  ELSE
    XF=XM2
    FF=F2
  END IF
210 CONTINUE
110 CONTINUE
510 CONTINUE
ZT2=XSOL
END IF
RETURN
END

C
C
C
C*****
C
C
C
C

FUNCTION EQCHAR(NM,NT,H,OM,XI,ZT1,ZT2)
IMPLICIT REAL*8 (A-H,O-Z)

```

C
C
C

```

PI=4. DO*DATAN(1. DO)
D=(FKZ(OM,XI,H)-FKZ(OM,XI,H-5. DO))/(10. DO*FKZ(OM,XI,H)**2)
IF (DABS(D). GT. . 999DO) THEN
  D1=(D/DABS(D))* . 999DO
ELSE
  D1=D
END IF

```

C
C
C

```

IF (NT. EQ. 1) THEN
  EQCHAR=PHASE(0. DO,ZT1,OM,XI)-(NM-. 25DO)*PI
  IF (H-ZT1. GT. 10. DO) THEN
    PHIB=PHASE(ZT1,H,OM,XI)-DATANH(D1)
    EQCHAR=EQCHAR+DATAN(DEXP(-2. DO*PHIB)/2. DO)
  ELSE
    GAM=(FKZ2(OM,XI,H)-FKZ2(OM,XI,ZT1))/(ZT1-H)
    ZH=(GAM/DABS(GAM))*DABS(GAM)**(1. DO/3. DO)*(H-ZT1)
    A=DBI(ZH)
    B=DAI(ZH)
    EQCHAR=EQCHAR-DATAN(B/A)
  END IF
ELSE IF (NT. EQ. 2) THEN
  EQCHAR=PHASE(ZT1,H,OM,XI)
  IF(ZT1. GT. 10. DO) THEN
    PHIS=PHASE(0. DO,ZT1,OM,XI)
    ALF1=DEXP(PHIS)+D*DEXP(-1. DO*PHIS)/2. DO
    ALF2=((DEXP(-1. DO*PHIS)/2. DO)-D*DEXP(PHIS))
    IF (DLOG10(DABS(ALF1))-DLOG10(DABS(ALF2)). GT. 60. DO) THEN
      IF (D. GE. 0) THEN
        ALF=PI/2. DO
      ELSE
        ALF=-1. DO*PI/2. DO
      END IF
    ELSE
      ALF=DATAN(ALF1/ALF2)
    END IF
    IF (D. GE. 0. DO) THEN
      EQCHAR=EQCHAR-(NM-1. 25DO)*PI+ALF
    ELSE
      EQCHAR=EQCHAR-(NM-. 25DO)*PI+ALF
    END IF
  ELSE
    GAM=(FKZ2(OM,XI,ZT1)-FKZ2(OM,XI,0. DO))/ZT1
    ZS=(GAM/DABS(GAM))*DABS(GAM)**(1. DO/3. DO)
    A=BI(ZS)
    B=AI(ZS)
    IF (D. LT. 0. DO) THEN
      EQCHAR=EQCHAR-(NM-. 25DO)*PI+DATAN((A+D*B)/(B-D*A))
    ELSE
      EQCHAR=EQCHAR-(NM-1. 25DO)*PI+DATAN((A+D*B)/(B-D*A))
    END IF
  END IF

```

```

      END IF
C
C
C
ELSE IF (NT.EQ.3) THEN
  IF (H-ZT2.GT.10.DO) THEN
    PHIB=PHASE(ZT2,H,OM,XI)-DATANH(D1)
    ALF2=DATAN(DEXP(-2.DO*PHIB)/2.DO)
  ELSE
    GAM=(FKZ2(OM,XI,H)-FKZ2(OM,XI,ZT2))/(ZT2-H)
    ZH=(GAM/DABS(GAM))*DABS(GAM)**(1.DO/3.DO)*(H-ZT2)
    A=DBI(ZH)
    B=-1.DO*DAI(ZH)
    ALF2=DATAN(B/A)
  END IF
  IF(ZT1.GT.10.DO) THEN
    PHIS=PHASE(0.DO,ZT1,OM,XI)
    ALF1=DATAN(DEXP(-2.DO*PHIS)/2.DO)
  ELSE
    GAM=(FKZ2(OM,XI,ZT1)-FKZ2(OM,XI,0.DO))/ZT1
    ZS=(GAM/DABS(GAM))*DABS(GAM)**(1.DO/3.DO)*ZT1
    A=BI(ZS)
    B=AI(ZS)
    ALF1=DATAN(B/A)
  END IF
  EQCHAR=PHASE(ZT1,ZT2,OM,XI)
  EQCHAR=EQCHAR-(NM-.5DO)*PI-ALF1+ALF2
C
C
C
ELSE
  EQCHAR=PHASE(0.DO,H,OM,XI)
  IF (DABS(D).GT.1.D-60) THEN
    E=1.DO/D
    IF(D.GT.0.DO) THEN
      EQCHAR=EQCHAR-NM*PI+DATAN(E)
    ELSE
      EQCHAR=EQCHAR-NM*PI-DATAN(E)
    END IF
  ELSE
    EQCHAR=EQCHAR-NM*PI+PI/2.DO
  END IF
C
C
C
END IF
C
RETURN
END
C
C
C
C*****
C
C
C

```

```

FUNCTION PHASE(A,B,OM,XKN)
IMPLICIT REAL*8 (A-H,O-Z)
XNL=DINT((B-A)/5.D0)
NL=NINT(XNL)
EX=DMOD((B-A),5.D0)
PHASE=0.D0
DO I=1,NL
  XI=DBLE(I)
  PHASE=PHASE+(FKZ(OM,XKN,(XI-1.D0)*5.D0+A)
$      +FKZ(OM,XKN,XI*5.D0+A))*2.5D0
END DO
PHASE=PHASE+(FKZ(OM,XKN,XNL*5.D0+A)
$      +FKZ(OM,XKN,B))*EX/2.D0
RETURN
END

```

C
C
C
C*****
C
C
C

```

FUNCTION FKZ(OM,XKN,Z)
REAL*8 FKZ,OM,XKN,Z
FKZ=(OM/C(Z))**2-XKN**2
FKZ=DSQRT(DABS(FKZ))
RETURN
END

```

C
C
C
C*****
C
C
C

```

FUNCTION FKZ2(OM,XKN,Z)
REAL*8 FKZ2,OM,XKN,Z
FKZ2=(OM/C(Z))**2-XKN**2
RETURN
END

```

C
C
C
C*****
C
C
C

```

FUNCTION C(Z)
REAL*8 C,Z
C=
RETURN
END

```

C
C
C
C*****

```

C
C
C
FUNCTION AI(Z)
IMPLICIT REAL*8 (A-H,O-Z)
REAL*8 J13,JM13,I13,IM13
DIMENSION RJ(2),WK(4),B(2)

C
C
C
IF (Z.EQ.0.D0) THEN
  AI=.35502805D0
  RETURN
ELSE IF (Z.LT.0.D0) THEN

C
C
C
  ARG=2.D0*(DSQRT(-1.D0*Z)**3)/3.D0
  N=2

C
C
C
  ORDER=2.D0/3.D0
  CALL MMBSJR(ARG,ORDER,N,RJ,WK,IER)
  JM13=4.D0*RJ(1)/(3.D0*ARG)-RJ(2)

C
C
C
  ORDER=1.D0/3.D0
  CALL MMBSJR(ARG,ORDER,N,RJ,WK,IER)
  J13=RJ(1)

C
C
C
  AI=DSQRT(-1.D0*Z)*(JM13+J13)/3.D0

C
C
C
  RETURN
  ELSE

C
C
C
  ARG=2.D0*(DSQRT(Z)**3)/3.D0
  ORDER=2.D0/3.D0
  NB=2
  IOPT=1

C
C
C
  CALL MMBSIR(ARG,ORDER,NB,IOPT,B,IER)
  IM13=4.D0*B(1)/(3.D0*ARG)+B(2)

C
C
C
  ORDER=1.D0/3.D0

```

```

      CALL MMBSIR(ARG,ORDER,NB,IOPT,B,IER)
      I13=B(1)
C
C
C
      AI=DSQRT(Z)*(IM13-I13)/3.D0
      RETURN
C
C
C
      END IF
C
C
C
      END
C
C
C
C*****
C
C
C
      FUNCTION BI(Z)
      IMPLICIT REAL*8 (A-H,O-Z)
      REAL*8 J13,JM13,I13,IM13
      DIMENSION RJ(2),WK(4),B(2)
C
C
C
      IF (Z.EQ.0.D0) THEN
        BI=.61492663D0
        RETURN
      ELSE IF (Z.LT.0.D0) THEN
C
C
C
        ARG=2.D0*(DSQRT(-1.D0*Z)**3)/3.D0
        N=2
C
C
C
        ORDER=2.D0/3.D0
        CALL MMBSJR(ARG,ORDER,N,RJ,WK,IER)
        JM13=4.D0*RJ(1)/(3.D0*ARG)-RJ(2)
C
C
C
        ORDER=1.D0/3.D0
        CALL MMBSJR(ARG,ORDER,N,RJ,WK,IER)
        J13=RJ(1)
C
C
C
        BI=DSQRT(-1.D0*Z/3.D0)*(JM13-J13)
C

```

```

C
C
    RETURN
    ELSE
C
C
C
    ARG=2. DO*(DSQRT(Z)**3)/3. DO
    ORDER=2. DO/3. DO
    NB=2
    IOPT=1
C
C
C
    CALL MMBSIR(ARG,ORDER,NB,IOPT,B,IER)
    IM13=4. DO*B(1)/(3. DO*ARG)+B(2)
C
C
C
    ORDER=1. DO/3. DO
    CALL MMBSIR(ARG,ORDER,NB,IOPT,B,IER)
    I13=B(1)
C
C
C
    BI=DSQRT(Z/3. DO)*(IM13+I13)
    RETURN
C
C
C
    END IF
C
C
C
    END
C
C
C
C*****
C
C
C
    FUNCTION DAI(Z)
    IMPLICIT REAL*8 (A-H,O-Z)
    REAL*8 J23,JM23,I23,IM23
    DIMENSION RJ(2),WK(4),B(2)
C
C
C
    IF (Z.EQ.0. DO) THEN
        DAI=-.25881940DO
        RETURN
    ELSE IF (Z.LT.0. DO) THEN
C
C
C

```

```

ARG=2. D0*(DSQRT(-1. D0*Z)**3)/3. D0
N=2
C
C
C
ORDER=1. D0/3. D0
CALL MMBSJR(ARG,ORDER,N,RJ,WK,IER)
JM23=2. D0*RJ(1)/(3. D0*ARG)-RJ(2)
C
C
C
ORDER=2. D0/3. D0
CALL MMBSJR(ARG,ORDER,N,RJ,WK,IER)
J23=RJ(1)
C
C
C
DAI=Z*(JM23-J23)/3. D0
C
C
C
RETURN
ELSE
C
C
C
ARG=2. D0*(DSQRT(Z)**3)/3. D0
ORDER=1. D0/3. D0
NB=2
IOPT=1
C
C
C
CALL MMBSIR(ARG,ORDER,NB,IOPT,B,IER)
IM23=2. D0*B(1)/(3. D0*ARG)+B(2)
C
C
C
ORDER=2. D0/3. D0
CALL MMBSIR(ARG,ORDER,NB,IOPT,B,IER)
I23=B(1)
C
C
C
DAI=-1. D0*Z*(IM23-I23)/3. D0
RETURN
C
C
C
END IF
C
C
C
END
C
C

```



```

C
C*****
C
C
C
FUNCTION DBI(Z)
IMPLICIT REAL*8 (A-H,O-Z)
REAL*8 J23,JM23,I23,IM23
DIMENSION RJ(2),WK(4),B(2)
C
C
C
IF (Z.EQ.0.D0) THEN
    DBI=.44828836D0
    RETURN
ELSE IF (Z.LT.0.D0) THEN
C
C
C
    ARG=2.D0*(DSQRT(-1.D0*Z)**3)/3.D0
    N=2
C
C
C
    ORDER=1.D0/3.D0
    CALL MMBSJR(ARG,ORDER,N,RJ,WK,IER)
    JM23=2.D0*RJ(1)/(3.D0*ARG)-RJ(2)
C
C
C
    ORDER=2.D0/3.D0
    CALL MMBSJR(ARG,ORDER,N,RJ,WK,IER)
    J23=RJ(1)
C
C
C
    DBI=-1.D0*Z*(JM23+J23)/DSQRT(3.D0)
C
C
C
    RETURN
    ELSE
C
C
C
    ARG=2.D0*(DSQRT(Z)**3)/3.D0
    ORDER=1.D0/3.D0
    NB=2
    IOPT=1
C
C
C
    CALL MMBSIR(ARG,ORDER,NB,IOPT,B,IER)
    IM23=2.D0*B(1)/(3.D0*ARG)+B(2)
C

```

```

C
C
ORDER=2. D0/3. D0
CALL MMBSIR(ARG,ORDER,NB,IOPT,B,IER)
I23=B(1)
C
C
C
DBI=Z*(IM23+I23)/DSQRT(3. D0)
RETURN
C
C
C
END IF
C
C
C
END

```

REFERENCES

Bender, C. M., and S. A. Orszag, *Advanced Mathematical Methods for Scientists and Engineers*, McGraw-Hill Inc., 1978.

Chiu, C.-S., and L. Ehret, *Computation of Sound Propagation in a Three-dimensionally Varying Ocean: A Coupled Normal Mode Approach*, Computational Acoustics, Vol. 1, Elsevier Science Publishers B. V., 1990.

Clay, C. S., and H. Medwin, *Acoustical Oceanography*, John Wiley & Sons Inc., 1977.

Gerald, C. F., and P. O. Wheatley, *Applied Numerical Analysis*, Addison-Wesley, 1989.

Kinsler, L. E., A. R. Frey, A. B. Coppens and J. V. Sanders, *Fundamentals of Acoustics*, John Wiley & Sons Inc., 1982.

Nayfeh, A. H., *Perturbation Methods*, John Wiley, 1973.

BIBLIOGRAPHY

Abramowitz, M., and I. A. Stegun, *Handbook of Mathematical Functions*, National Bureau of Standards, 1964.

Apel, J. R., *Principles of Ocean Physics*, Academic Press Lim., 1988.

Beyer, W. H. (Editor), *CRC Standard Mathematical Tables*, CRC Press, 1981.

Butkov, E., *Mathematical Physics*, Addison-Wesley Publishing Company Inc., 1968.

Hamilton, E. L., *Geoacoustic Modeling of the Ocean Floor*, Journal of the Acoustical Society of America, Vol. 68, No. 5, 1980.

Lighthill, J., *Waves in Fluids*, Cambridge University Press, 1978.

Murphy, E. L., and J. A. Davis, *Modified Ray Theory for Bounded Media*, Journal of the Acoustical Society of America, Vol. 56, No. 6, 1974.

Nyhoff, L., and S. Leestma, *FORTRAN 77 for Engineers and Scientists*, Macmillan Publishing Company, 1988.

Urick, R. J., *Principles of Underwater Sound*, McGraw-Hill Inc., 1983.

INITIAL DISTRIBUTION LIST

	No. Copies
1. Defense Technical Information Center Cameron Station Alexandria, VA 22304-6145	2
2. Library, Code 52 Naval Postgraduate School Monterey, CA 93943-5002	2
3. Chairman (Code OC/Co) Department of Oceanography Naval Postgraduate School Monterey, CA 93943	1
4. LT Fernando M. M. Pimentel Instituto Hidrografico Rua das Trinas 1200 Lisboa Portugal	2
5. Dr. C.-S. Chiu (Code OC/Ci) Department of Oceanography Naval Postgraduate School Monterey, CA 93943	2
6. Ms. L.L. Ehret (Code OC/Eh) Department of Oceanography Naval Postgraduate School Monterey, CA 93943	1
7. Naval Oceanographic Office Stennis Space Center Bay St. Louis, MS 39522	1
8. Direccao do Servico de Instrucao e Treino Marinha Portuguesa Rua do Arsenal 1100 Lisboa Portugal	1
9. Director Geral do Instituto Hidrografico Instituto Hidrografico Rua das Trinas, 49 1200 Lisboa Portugal	2